Aus dem Institut für Schlaganfall- und Demenzforschung

der Ludwig-Maximilians-Universität München

Direktor: Prof. Dr. med. Martin Dichgans

Role of the Large Vessel Stroke Relevant Gene HDAC9 in NF-κB Activation and Atherogenic Processes in Vascular Cells.

Dissertation

zum Erwerb des Doktorgrades der Medizin

an der Medizinischen Fakultät der

Ludwig-Maximilians-Universität zu München

vorgelegt von

Yury Bokov

aus

Moskau, Russland

2022

Mit Genehmigung der Medizinischen Fakultät
der Universität München

Berichterstatter:	Prof. Dr. med. Martin Dichgans
Mitberichterstatter:	Prof. Dr. rer. nat. Alexander Bartelt
	PD Dr. rer. nat. Andreas Herbst
Mitbetreuung durch den promovierten Mitarbeiter:	Dr. rer. nat. Yaw Asare
Dekan:	Prof. Dr. med. Thomas Gudermann
Tag der mündlichen Prüfung:	28.04.2022

Table of Contents

Part of the results have been published in:

Asare Y, Campbell-James TA, **Bokov Y**, Yu LL, Prestel M, El Bounkari O, Roth S, Megens RTA, Straub T, Thomas K, Yan G, Schneider M, Ziesch N, Tiedt S, Silvestre-Roig C, Braster Q, Huang Y, Schneider M, Malik R, Haffner C, Liesz A, Soehnlein O, Bernhagen J, Dichgans M. **Histone Deacetylase 9 Activates IKK to Regulate Atherosclerotic Plaque Vulnerability.** Circ Res. 2020 Aug 28;127(6):811-823.

Abbreviations

ACA	Anterior cerebral artery
ApoE	Apolipoprotein E
BrdU	5-brom-2'deoxyuridine
BSA	Bovine serum albumin
CAD	Coronary artery disease
CBF	Cerebral blood flow
CCA	Common carotid artery
CCL2	CC chemokine ligand 2
Cdk	Cyclin-dependent kinase
cDNA	Complementary DNA
DALY	Disability adjusted life years
DNA	Deoxyribonucleic acid
EC	Endothelial cell
ELISA	Enzyme linked immunosorbent assay
ERK	Extracellular signal-regulated kinases
FoxP3	Forkhead box P3
GAPDH	Glyceraldehyde 3 phosphate dehydrogenase
GWAS	Genome-wide association study
HAT	Histone acetyltransferase
HAoSMC	Human aortic smooth muscle cell
HDAC	Histone deacytelase
HDAC9	Histone deacetylase 9
HUVEC	Human umbilical vein endothelial cells
ICAM-1	Intercellular adhesion molecule 1
IFN	Interferon
IL-8	Interleukin 8
IκB-α	Inhibitor kappa B-alpha
IKK	Inhibitor kappa B kinase
JNK	cJun NH2-terminal kinases
LAS	Large Artery Stroke
LDL	Low density lipoprotein
LDLR	Low density lipoprotein receptor

LFA1	Lymphocyte function associated antigen
LVS	Large vessel stroke
MAPK	Mitogen-activated proliferation kinase
MCP-1	Monocyte chemoattractant protein-1
MI	Myocardial infarction
NF-κB	Nuclear factor 'kappa-light-chain-enhancer' of activated B-cells
oxLDL	Oxidized LDL
PDGF	Platelet derived growth factor
PDGF-Rβ	PDGF receptor beta
PFA	Paraformaldehyde
ROI	Region of interest
RNA	Ribonucleic acid
SCR	Scramble control
siRNA	Small interfering RNA
SMC	Smooth muscle cell
SNP	Single nucleotide polymorphism
SOCS1-ECS	Suppressor of cytokine signaling 1
TGF	Transforming growth factor
TNF-α	Tumor necrosis factor-alpha
TNFR1	Tumor necrosis factor receptor 1
TOAST	Trial of organization 10172 in acute stroke treatment
TPL2	Tumor progression Locus 2
Tregs	Regulatory T cells
VCAM-1	Vascular cell adhesion molecule 1
VLA4	Very late antigen 4
VSMC	Vascular smooth muscle cell
WT	Wild type

Summary

Genome-wide association studies identified histone deacetylase 9 (HDAC9) gene region as the strongest risk locus for large vessel stroke (LVS) and a major locus for coronary artery disease (CAD). Substantial advances in our understanding of atherosclerotic plaque formation aid deciphering the complex pathogeneses of both LVS and CAD. In essence, atherosclerosis is a chronic inflammatory disorder of the vascular wall orchestrated by an interplay of vascular resident and immune cells. An insult to the vascular wall results in the production of chemokines and adhesion molecules, leading to lipid-deposition and plaque formation at the lesion site. With these mechanisms in mind, our group recently reported Hdac9-deficiency to attenuate atherosclerosis in ApoE-deficient mice. However, the mechanisms underlying the proatherogenic effect of HDAC9 remain unknown. It is important to consider that previous data already showed HDAC9 to be ubiquitously expressed in endothelial (EC) and smooth muscle cells (SMC). Hence, elucidating the role of these cell types could expand our knowledge about HDAC9-mediated atherogenesis and provide novel precision medicine approaches for LVS.

In this thesis we aimed to: (1) examine HDAC9-mediated effects on proatherogenic molecules (VCAM-1, ICAM-1, MCP-1/CCL2 and IL-8) in HDAC9-deficient ECs and SMCs stimulated by TNF-α and measure the production of the same chemokines and adhesion molecules in Apoe-/-Hdac9-/- mice; (3) investigate the mechanism linking HDAC9 to pro-inflammatory responses; (4) analyze changes to SMC proliferation affected by reduced HDAC9 expression.

Using RT-PCR und western blot, we detected reduced mRNA expression and protein levels of VCAM-1, ICAM-1, MCP-1/CCL2 and IL-8 upon TNF-α stimulation in ECs and SMCs transiently transfected with HDAC9 siRNA. Double knockout Apoe-/-Hdac9-/- mice which were fed a lipid-rich diet showed reduced levels of circulating Ccl2, Vcam-1 as well as Icam-1 in whole-aorta lysates. Interestingly, adhesion molecule levels were also reduced in single-knockout Hdac9-

deficient mice which were fed the same lipid-rich diet. This emphasizes the sole importance of the Hdac9 gene for

proatherogenic molecule production.

In order to understand how HDAC9 controls proinflammatory molecule production, we explored the underlying mechanisms that lead to expression of these proteins. NF-κB transcriptional activity was measured with a luciferase reporter gene assay and phosphorylation of p65 at Ser468 and Ser536 was detected using western blot. Analysis of nuclear and cytoplasmic p65 levels in ECs that underwent HDAC9 knockdown was also carried out. Our findings demonstrated HDAC9 to enhance NF-κB activity, promote efficient p65 nuclear translocation and be essential for sustained phosphorylation at Serine 536 and 468 in both ECs and SMCs. Additionally, HDAC9-mediated effects on two main MAPK signaling pathways were investigated and phosphorylation of p38 and ERK1/2 was shown to be unaffected upon HDAC9 knockdown. Lastly, effects of HDAC9 knockdown on SMC proliferation were investigated. Our data showed a 50% decrease in BrdU incorporation as well as CyclinD1 levels in HDAC9-deficient SMCs stimulated by PDGF-BB and TNF-α.

In light of this data following conclusions can be made: (1) HDAC9 enhances the production of proatherogenic molecules (VCAM-1, ICAM-1, MCP-1/CCL2, IL-8) in EC and SMCs as well as Ccl2, Vcam-1 and Icam-1 in atherosclerosis-prone mice; (2) HDAC9 increases pro-inflammatory responses by enhancing NF-κB transcriptional activity and p65 nuclear translocation; (3) HDAC9 is essential for SMC proliferation in a proinflammatory milieu.

In summary, we provide new data that expands our understanding of how HDAC9 mediates atherosclerotic plaque formation and increases LVS risk. Finally, we discuss the use of a specific HDAC9 inhibitor as a promising new target-based approach to decrease the development of atherosclerosis by suppressing vascular inflammation.

Zusammenfassung

Genom-weite Assoziationsstudien identifizierten Histon Deacetylase 9 (HDAC9) Genregion als den höchsten Risikolocus für den ischämischen Schlaganfall der großen hirnversorgenden Arterien und den Hauptrisikolocus für koronare Herzerkrankung. Erhebliche Fortschritte im Verständnis der atheroskleroticschen Plaquebildung helfen bei der Entschlüsselung der komplexen Pathogenese sowohl des LVS als auch der KHK. Atherosklerose ist eine chronische Entzündung der Gefäßwand, die durch das Zusammenspiel von Gefäß- und Immunzellen verursacht wird. Eine Reizung der Gefäßwand bewirkt die Produktion von Chemokinen und Adhäsionsmolekülen, die dann zu Lipidablagerung und schließlich zu Plaquebildung an der Läsionsstelle führen. Erst kürzlich gab unsere Arbeitsgruppe bekannt, wie Atherosklerose bei Apoe-/- Mäusen durch Hdac9-Knockout verhindert werden kann. Die Mechanismen, die der proatherogenen Wirkung von HDAC9 zugrunde liegen, sind jedoch unklar. Aufgrund der ubiquitären HDAC9-Expression in den Zellen des Endothels und der glatten Muskulatur, ist weitere Analyse der zellspezifischen Rollen erforderlich, um die HDAC9-mediierte Atherogenese zu verstehen. Durch diese Erkentnisse würde eine Möglichkeit entstehen, gezielte Therapieoptionenen für den makroangiopathischen ischämischen Schlaganfall zu entwickeln.

Die Ziele dieser Arbeit waren: (1) Die Untersuchung der HDAC9-mediierten Effekte auf proatherogene Moleküle (VCAM-1, ICAM-1, MCP-1 / CCL2 und IL-8) in TNF-α stimulierten HDAC9-defizienten ECs und SMCs und die Ermessung der gleichen Chemokine und Adhäsionsmoleküle in Apoe-/-Hdac9-/- Mäusen;

(2) Die Verlinkung von HDAC9 als mechanistischer Mediator in einem proatherogenen Signalweg;

(3) Die Analyse der geminderten HDAC9-Expression auf SMC-Proliferation.

Die Analyse der mRNA-Expression und der Proteinmenge mit RT-PCR und Western Blot zeigte eine Reduktion der VCAM-1, ICAM-1, MCP-1 / CCL2 und IL-8 nach einer TNF-α-Stimulation in HDAC9-defizienten ECs und SMCs. Ein niedriger Spiegel an zirkulierendem CcI2 sowie aortalen Vcam-1 und Icam-1 konnte bei den Apoe-/-Hdac9-/- Mäusen festgestellt werden, denen eine

lipidreiche Kost verabreicht wurde. Zudem sahen wir eine Verminderung der gleichen Adhäsionsmoleküle bei Mäusen mit alleiniger Hdac9-Genstillegung, die eine lipidbilanzierte Kost erhielten. Diese Erkenntnisse belegen die individuelle Zuständigkeit des Hdac9-Gens für die Synthese proatherogener Moleküle.

Um die zugrunde liegenden Mechanismen dieser HDAC9-kontrollierten Effekte bestimmen zu können, analysierten wir die Transkriptionsaktivität von NF-κB mit Luciferase-Reportergen-Assay sowie die Phosphorylierung von p65 auf Ser468 und Ser536 mit Western Blot. Zusätzlich untersuchten wir nukleare und zytoplasmatische p65-Spiegel in HDAC9-defizienten ECs. Als Ergebnis ließ sich eine Erhöhung der NF-κB-Aktivität durch HDAC9 festhalten. Darüber hinaus hielt HDAC9 die erfolgreiche p65-Kerntranslokation sowie die Phosphorylierung an Serin 536- und 468 sowohl in Endothel- als auch in glatten Muskelzellen aufrecht.

Anschließend betrachteten wir zwei wichtige MAPK Signalwege, um weitere mögliche HDAC9-mediierte Effekte zu identifizieren. Die Phosphorylierung von p38 und ERK1/2 blieb beim HDAC9-Knockdown unverändert. Schließlich prüften wir die Auswirkungen des HDAC9-Knockdowns auf die SMC-Proliferation. Hier demonstrierten HDAC9-defiziente SMCs eine ca. 50%-ige Senkung der BrdU-Inkorporation und des CyclinD1-Spiegels nach Stimulation mit PDGF-BB und TNF-α.

Anhand dieser Ergebnisse lässt sich schlussfolgern: (1) Die Transkription von VCAM-1, ICAM-1, MCP-1/CCL2 und IL-8 in vitro sowie Ccl2, Vcam-1 und Icam-1 in vivo durch HDAC9 induziert wird; (2) HDAC9 erhöht pro-inflammatorische Reaktionen durch Steigerung der NF-κB-Transkriptionsaktivität und p65-Kerntranslokation;

(3) SMC-Proliferation ist im proinflammatorischen Milieu stark von HDAC9 abhängig.

Zusammenfassend konnten wir HDAC9 als einen wichtigen Mediator des NF-κB Signalwegs identifizieren, der für die Initiierung und Entwicklung von Atherosklerose ausschlaggebend ist.

Um die Entwicklung neuer zielbasierter Therapien für die effektive Unterdrückung der Gefäßentzündung einsetzen zu können, ist es entscheidend, dass unser Verständnis für diesen Pathomechanismus stets erweitert wird.

1. Introduction

1.1 Stroke

1.1.1 Epidemiology

Stroke is a major cause of death worldwide[1]. Half of stroke patients are left chronically disabled, ranking it second-highest in total disability adjusted life years (DALYs)[2]. Existing evidence shows incidence of stroke to increase with age and double for every decade after the age of 55[3]. Between 1993 and 2005 mean age at stroke fell from 71.2 to 69.2 years, while global average life expectancy rose by 5.5 years in the last two decades[4]. Despite this development death rate of stroke continues to decline due to on-going improvements of treatment strategies[3,4,5]. Unfortunately, surviving cerebral ischemia also means more people live with post-stroke consequences. In 2017, EU total economic cost of stroke estimated at whopping €57 billion and are set to rise in the future[6,7]. These trends emphasize the growing burden of stroke on public health and healthcare systems due to demographic transitions of populations. To tackle this problem, scientific research began focusing on identifying risk factors contributing to stroke.

Risk factors are defined as modifiable or non-modifiable for both primary and recurrent stroke[8]. A recent international case-control study INTERSTROKE listed 10 modifiable factors, which are attributed 90% of risk for stroke[8]. These include hypertension, high blood cholesterol, smoking, diabetes, alcohol consumption, heart disease, obesity, poor diet and sedentary lifestyle. Nonetheless, the search now continues for novel risk factors that contribute to the pathophysiology of specific stroke sub-types.

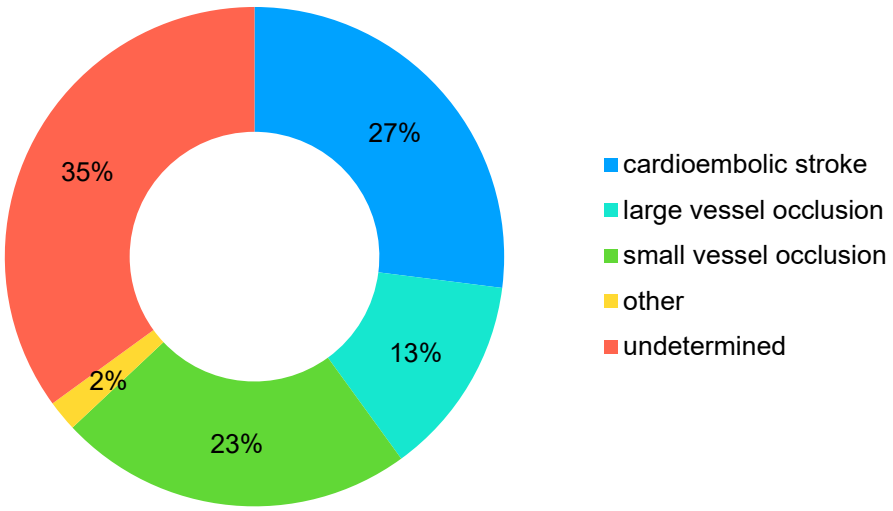

Figure 1. Etiology of Ischemic Stroke. Shown are percentages of stroke subtypes including: cardioembolic stroke (27%), large vessel stroke (13%), small vessel stroke (23%), other (2%) und undetermined (35%). Frequencies are taken from Kolominsky-Rabas et al.[9]

Ischemia is the underlying cause in 87% of overall stroke cases[9]. Five main types of ischemic stroke are classified by "Trial of Org 10172 in Acute Stroke Treatment" (TOAST) criteria: large vessel stroke (LVS), small artery occlusion (lacunar stroke), cardio-embolism and strokes of other determined or undetermined (cryptogenic) etiologies[10]. In cardioembolic stroke, a thrombus forms in the heart and blocks a distal artery in the brain. When small arteries are occluded, blood supply is restricted to subcortical or brainstem regions resulting in lacunar infarcts, typically <1.5cm in diameter. In LVS, atherosclerotic plaques lead to a significant stenosis (>50%) in one of cortical branch or primary brain arteries. Supporting vascular imaging of intra- or extracranial arteries would reveal plaques in atherosclerosis-prone sites, such as carotid artery bifurcation. Neurons are particularly vulnerable to hypoxic and hypoglycemic damage implicated by insufficient perfusion. As a result, branch or large hemispheric, brain stem, or cerebellar infarction in LVS usually causes severe neurological functional deficits. For most patients, neurorehabilitation after a major ischemic event is a long and tedious process that does not guarantee complete recovery of function and varies between each individual. Thus, understanding risk factors deeply embedded in our DNA could be a game changer in developing targeted approaches for preventing and treating LVS.

1.1.2 Stroke Genetics and Genome-Wide Association Studies

Ischemic stroke is attributed to a wide range of modifiable and non-modifiable risk factors[8]. Uncontrollable factors like genetics are responsible for a large proportion of stroke risk. In fact, heritability for all ischemic stroke was 37,9% and 40,3% specifically for large vessel stroke[11]. These genetic predispositions are classified as either a single or multiple gene disorder. Even though polygenic contribution to the heterogeneous etiopathogenesis of stroke is complex, identifying specific genetic variants could facilitate further stroke subtyping, while elucidating gene regulatory mechanisms may yield novel targets for precision medicine approaches[12,13].

Genome-wide association studies (GWAS) compare entire genomes of cases and controls to identify common (frequency>1%) genetic variants[14]. More specifically, a variation in a single nucleotide (Single Nucleotide polymorphism, SNP) is associated with a trait. As more low-cost sequencing technologies become available, new genome-wide genotyping enables rarer variants to be identified[13]. Many stroke risk SNPs to date associate with common vascular risk factors like hyperlipidemia or confer overlapping risk to related pathologies like coronary artery disease[15,16]. This and large sample sizes are clear advantages that deem GWAS a highly promising approach for identifying novel risk loci[14].

In large vessel stroke (LVS), SNP rs2107595 at the HDAC9 locus on chromosome region 7p21.1 demonstrated the strongest association signal[17,18]. In the MEGASTROKE collaboration, HDAC9 reached a genome-wide significance (p-value= 3.65x10-8) from a data-set with >67,000 stroke cases and >450,000 controls[19]. The odds ratio was 1.21 (1.15-1.26) and the risk allele frequency was 24%.

The exact same HDAC9 risk locus was also identified in coronary artery disease (CAD) and myocardial infarction (MI)[20]. We already know that atherosclerosis is the common underlying cause of cerebral and cardiac ischemia. In fact, our group previously demonstrated Hdac9

deficiency to diminish plaque formation in atherosclerosis-prone mice[21]. Thus, further work in animal and cellular models is required to derive HDAC9-mediated mechanisms contributing to atherogenesis.

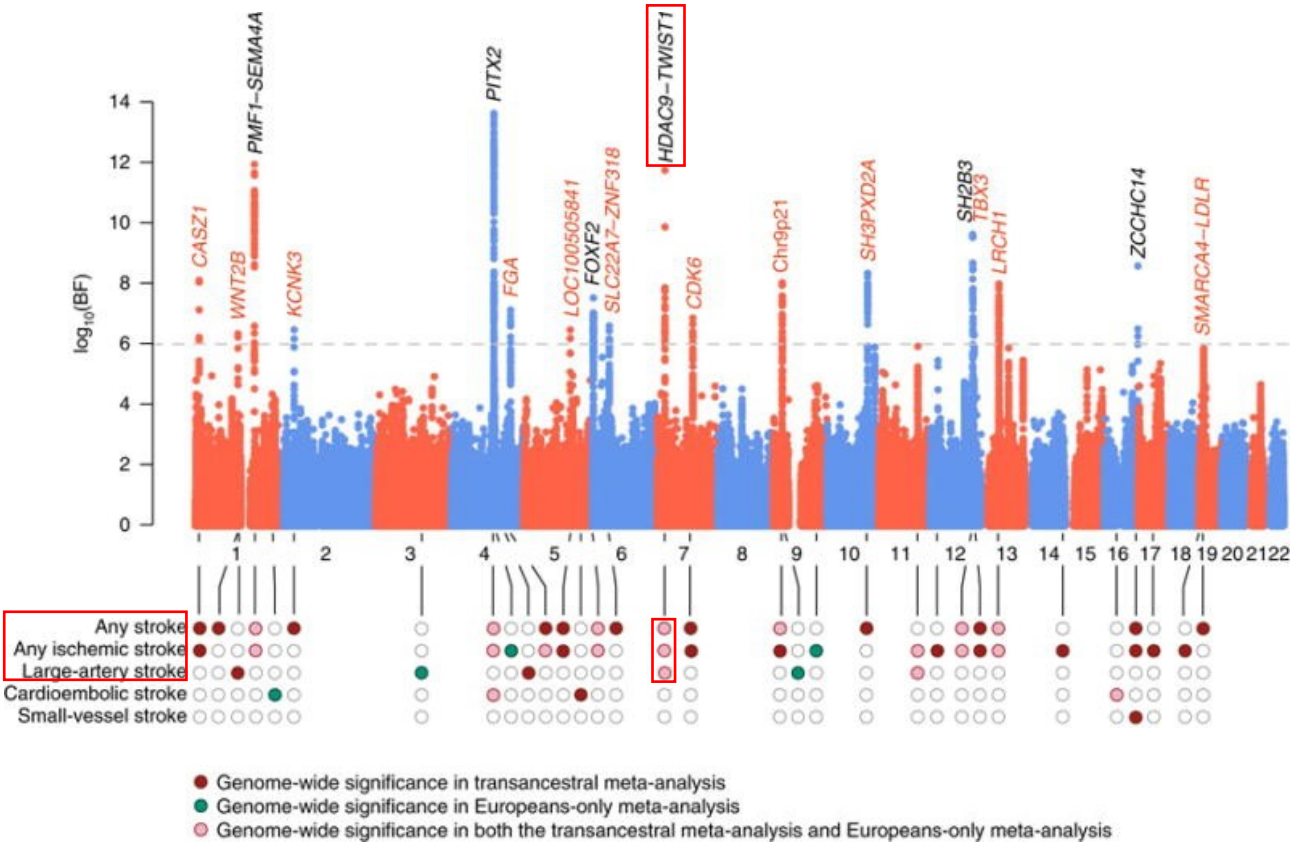

Figure 2. HDAC9 is the strongest signal for large artery atherosclerotic stroke. Manhattan blot from the latest GWAS on stroke with >520.000 individuals studied identifies 22 novel stroke risk loci and confirms HDAC9 as the strongest signal for large artery atherosclerotic stroke. Adapted from Malik R et al.[19]

1.2 Atherosclerosis

Atherosclerosis is the primary cause of coronary artery disease (CAD) and a major cause of stroke[22,23]. It is defined as a chronic autoimmune disease due to the involvement and regulation by both innate and adaptive immune systems[24]. Hypertension and high blood lipids are key players in the pathophysiology of this progressive inflammatory disorder[25]. The hallmark of atherosclerosis is plaque formation by long-term deposition of lipids, immune cells and calcium in a chronically insulted vascular wall[25,26]. It all begins with an endothelial injury triggering the infiltration of low density lipoproteins (LDL) into the intima, where oxidation to oxLDL takes places[27,28]. oxLDL´s immunogenicity activates a cascade of inflammatory processes and production of molecules involved in different stages of atherogenesis[28]. Initially, monocytes are recruited into the vascular endothelium and then differentiate into macrophages[29]. The latter take in oxLDL, become lipid-laden foam cells and form subendothelial fatty streaks, which are characteristic for early stages of atherogenesis[29]. As foam cells die, leukocytes surround the lipid-rich necrotic core. In advanced lesions, the extracellular matrix and smooth muscle cell media-to-intima migration and proliferation contribute to fibrous cap formation. The thickness of the fibrous cap and the degree of cap inflammation is responsible for the integrity and stability of the plaque[31,32]. As more VSMCs die, less proliferate, resulting in reduced plaque repair and insufficient synthesis of the extracellular matrix[33]. Two possible plaque complications are stenosis and rupture[34]. Usually, plaques are asymptomatic unless the cross-sectional area of the artery is significantly reduced to obstruct blood flow[34]. Most plaque ruptures are subclinical as complex plaques show signs of repeated rupture and repair[33,34]. Whether its significant luminal narrowing or plaque rupture, which lead to a local thrombus or embolic occlusion of distal arteries, the worst possible outcomes for both are myocardial infarction and stroke[33]. However, the mechanistic interplay in these complex disease events is not entirely understood and is still being investigated[35]. Adhesion molecules and chemokines play a pivotal role in initiating and sustaining vascular inflammation. Additionally, they

guard cellular processes like proliferation and apoptosis which contribute to plaque size and stability. Thus, studying this intricate intermolecular language to understand each message could help us inhibit or even reverse processes leading to stroke.

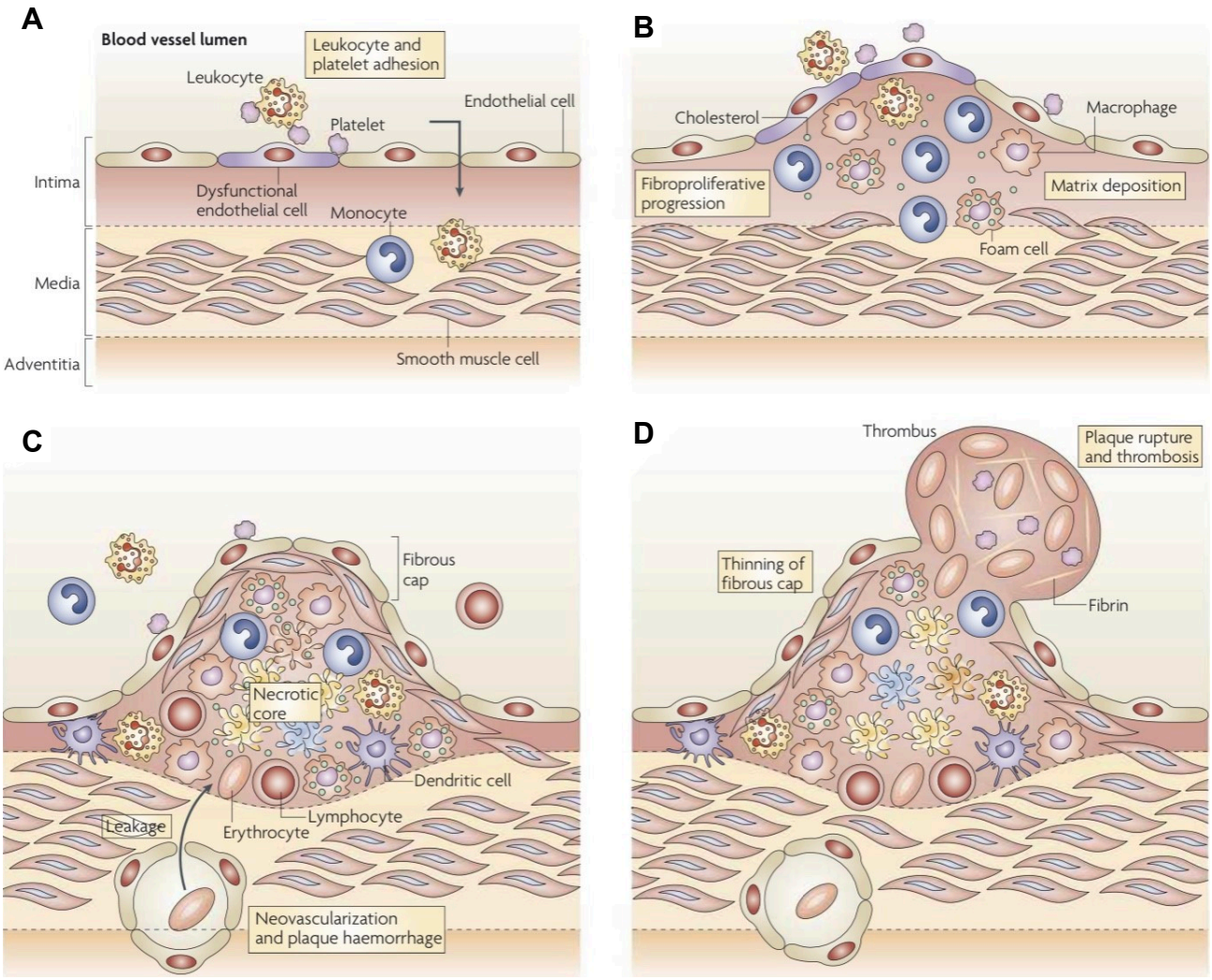

Figure 3. Development of Atherosclerosis. (A) Elevated serum lipids induce a proinflammatory milieu. Damaged endothelium results in increased retention of platelets and leukocytes, and their subsequent diapedesis into the intima. (B) Fatty streaks are made up of activated monocytes that differentiated into macrophages (foam cells) via rapid lipid-intake. A hallmark of atherosclerotic lesions is the accumulation of monocytes and SMCs as well as the dumping of matrix material to promote proliferation and fibrous cap formation. (C) In the plaque increased SMC proliferation and fibrous cap formation can be observed. A high rate of dying macrophages majorly contributes to the necrotic core found at the epicenter of the lesion. Recurrent bleeding and blood vessel formation can be found at the lesion site. (D) Structural integrity of the plaque is compromised via proteasomal degradation of the matrix and the destruction of the fibrous cap. Subsequently, a plaque rupture causes the activation of the coagulation cascaded that leads to thrombosis. Adapted from Weber C et al.[32]

1.2.1 Adhesion Molecules and Chemokines in Atherosclerosis

Atherosclerotic lesion formation is caused by chronically damages arterial intima and the release of proinflammatory TNF-α, which potentiates endothelial permeability[27,32]. More specifically, endothelially bound TNF-α induces the destabilization of the cytoskeleton and increases intercellular gaps for LDL transcytosis[27,28]. Increased concentrations of LDL and TNF-α amplify the expression of many proatherogenic adhesion molecules and chemokines by activation of signaling pathways involving NF-κB, p38-MAPK and extracellular signal-regulated kinase (ERK)[24,25,36]. Some of these molecules are VCAM-1, ICAM-1, CCL2/MCP-1 and IL-8.

Vascular and intercellular adhesion molecules (VCAM-1, ICAM-1) are two structurally and functionally related proteins of the Ig gene superfamily[37]. Usually within 30-120 mins of TNF-α stimulation, *de novo* synthesis of VCAM-1 and ICAM-1 is initiated[37]. To ensure robust adhesion, late antigen (VLA4) and lymphocyte function associated antigen (LFA1) found on monocytes bind to endothelial VCAM-1 and ICAM-1 respectively[37]. In hypercholesterolemic animals, VCAM-1 expression was limited to lesion and lesion-prone sites[38]. Reducing VCAM-1 levels actually attenuated early lesion formation by reducing monocyte rolling and adhesion in the aorta and carotid arteries[38]. In contrast, ICAM-1 deficient mice reduced aortic lesion progression and decreased development of advanced atherosclerotic plaques[39]. These studies demonstrated altering roles of VCAM-1 and ICAM-1 in different stages of atherosclerosis.

Chemokines like CC-chemokine ligand 2 (CCL2)/monocyte chemoattractant protein-1 (MCP-1) and Interleukin-8 (IL-8) are small cytokines that mediate cell migration and attraction[40,41]. Soluble CCL2/MCP-1 facilitates transendothelial migration by structurally changing monocytic cytoskeletons[42]. Additionally, CCL2/MCP-1 is responsible for SMC phenotypic switching, which plays a major role in neointima formation and restenosis[42]. In fact, patients with genetic predisposition to higher circulating CCL2/MCP-1 had increased risk for all ischemic and large vessel strokes[43]. Similarly, human atherosclerotic lesions reveal elevated IL-8[40]. Quantification of

IL-8

by ELISA demonstrated higher IL-8 levels in fibrous plaques compared to normal intima[40]. Further studies also implicate elevated IL-8 concentrations to increased SMC proliferation and enhanced angiogenesis in plaques[44]. Additionally, several clinical observational studies showed IL-8 levels in human serum to be the only marker that independently predicts cardiovascular events[40]. Furthermore simvastatin is an established prophylactic medication for ischemic stroke which exerts its atheroprotective effects by downregulating IL-8 secretion[45].

If one looks at more advanced lesions, VSMC differentiation, proliferation and migration are important processes contributing to plaque stability[46]. Platelet-derived growth factor (PDGF) is a disulphide-linked homodimeric mitogen that plays a major role in these processes[47]. PDGF family of proteins consists of 5 isoforms, however only those with two A (PDGF-AA) or two B (PDGF-BB) subunits are considered functional[47]. PDGF-BB binds with higher affinity to PDGF receptor beta (PDGFRβ) and is described to be one of the most important stimulants for VSMC function in atherosclerosis[48]. A recent study reveals suppression of PDGF-BB by inhibitor chicoric acid (CA) to induce atheroprotective responses[48]. More specifically, PDGF-BB depletion attenuated phenotypic switching, proliferation and migration in VSMCs by reducing p65 nuclear translocation in NF-κB signaling. Advanced atherosclerotic plaques are characterized by poor VSMC proliferation and extended population doubling times[34]. Decreased VSMC proliferation rate is attributed to an altered expression of various cell cycle regulators that drive G1/S phase transition[34,50]. Cyclins are eukaryotic proteins that form enzymatic complexes with cyclin dependent kinases (Cdk) in order to control cell cycle progression[51,52]. One example is cyclin D_1, which forms cyclinD_1:cdk4/6 complexes in proliferating cells[52]. Thus, observed reduction of cyclin D_1 expression in human plaque VSMCs indicates diminished cell replication[52].

In summary, adhesion molecules and chemokines are important mediators that initiate and drive atherosclerotic development. The synthesis of these molecules begins in the nucleus and is initiated by important gene factors like NF-κB. Exploring the function of these upstream regulators could unravel the answer to suppressing inflammation.

1.3 NF-κB is a Central Regulator of Vascular Inflammation

For over 30 years NF-κB (nuclear factor 'kappa-light-chain-enhancer' of activated B-cells) and TNF family of cytokines are a topic of tightly intertwined research[53]. NF-κB is a homo- or heterotrimeric protein complex of inducible transcription factors that plays a vital role in our immune system[54]. Five different proteins: p65 (RelA), RelB, c-Rel, p105/p50 (NF-κB1), and p100/52 (NF-κB2) belong to the NF-κB family and share a common N-terminal Rel homology domain (RHD)[53]. (Figure 4)

A typical p65:p50 heterodimer undergoes nuclear translocation where it binds to DNA via its RHD[53]. The transactivation domain found on p65 is a key feature which enables alterations to NF-κB transcriptional activity by co-activators and co-repressors[53,55,56]. TNF-α is historically known as cachexin due to its cachexia-inducing effect in some diseases. A variety of cell functions like differentiation, proliferation and apoptosis rely on TNF-mediated signaling[57].

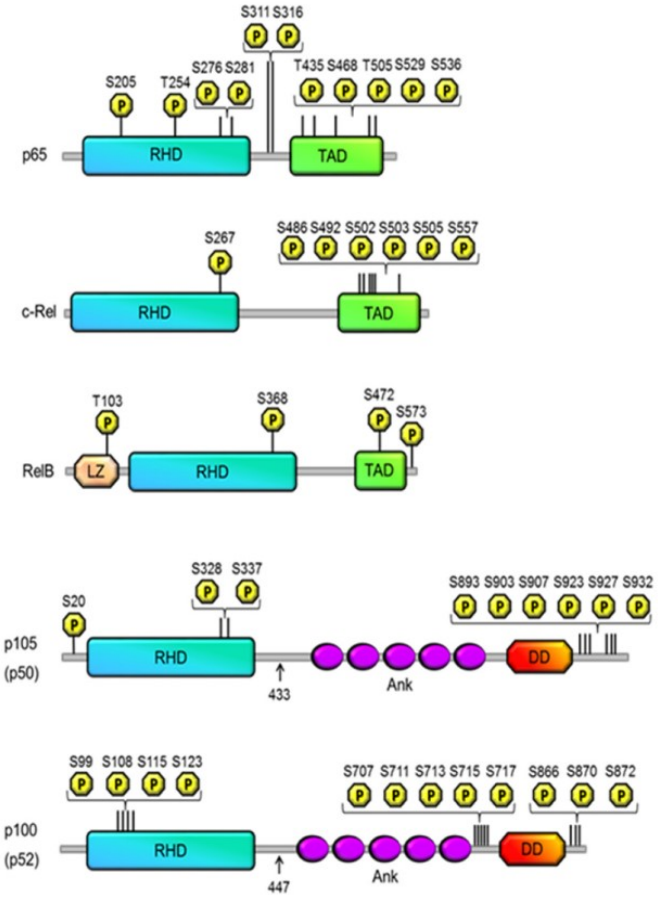

Figure 4. Phosphorylation of the NF-κB subunits. Illustrated is the NF-κB family: p65 (RelA), RelB, c-Rel, p100 (p52) and p105 (p50). C-terminal residues of p50 and p52 are shown by arrows. These are produced as a product of p105 and p52 processing. The main structural components for every subunit are depicted: REL homology domain (RHD); transactivation domain (TAD); ankyrin repeat domain (Ank); death domain (DD) and leucine zipper domain (LZ). NF-κB activation is guarded by the phosphorylation of particular serine sites, which are accurately shown respective to their structural location to each domain. Adapted from Hayden MS, Ghosh S.[53]

TNF-α plays a critical role in the pathogenesis of various diseases by regulating inflammatory responses[57]. Two receptors of the TNF receptor superfamily are ubiquitously expressed: TNFR1 immune cell restricted TNFR2. Depending on the stimulus, either a classical/canonical or alternate/non-canonical activation of NF-κB takes place[53]. TNFR1 ligation by soluble TNF-α activates the canonical NF-κB pathway[53]. TRADD recruits TRAF2 to TNFR1 forming Complex 1[54]. Robust NF-κB activation is ensured by Complex 1-mediated activation of the heterotrimer Inhibitor kappa B kinase (IKK) complex[54]. Resting cytotoxic state of a p65:p50 dimer complex is enforced by Inhibitor of kappa B alpha (IκB-α)[58]. A series of phosphorylations leads to activation of catalytic beta subunit (IKKβ) which marks the destruction box motif (DSGXXS) of IκB-α for degradative polyubiquination[58]. This process is complete within 10 minutes after TNF stimulation.

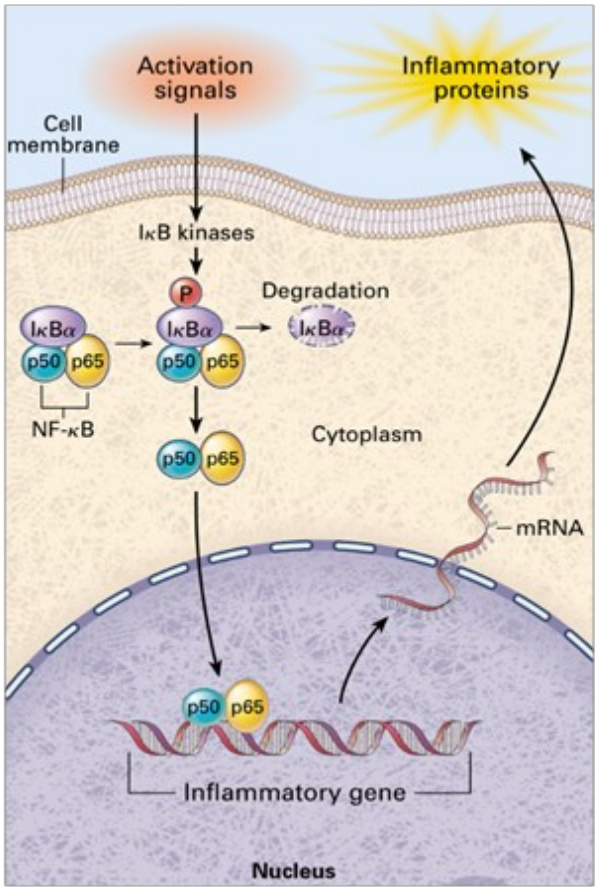

PROTEINS REGULATED BY NF-κB

Proinflammatory cytokines
Tumor necrosis factor α
Interleukin-1β
Interleukin-2
Interleukin-6
Granulocyte–macrophage colony-stimulating factor
Macrophage colony-stimulating factor
Granulocyte colony-stimulating factor

Chemokines
Interleukin-8
Macrophage inflammatory protein 1α
Macrophage chemotactic protein 1
Gro-α, -β, and -γ
Eotaxin

Inflammatory enzymes
Inducible nitric oxide synthase
Inducible cyclooxygenase-2
5-Lipoxygenase
Cytosolic phospholipase A_2

Adhesion molecules
Intercellular adhesion molecule 1
Vascular-cell adhesion molecule 1
E-selectin

Receptors
Interleukin-2 receptor (α chain)
T-cell receptor (β chain)

Figure 5. Schematic Diagram of NF-κB Activation and List of Proteins Regulated by NF-κB. NF-κB activation is initiated once IκB is marked for proteolytic degradation by its specific phosphorylating kinases. Subsequently, the p50:p65 heterodimer moves into the nucleus. As a result, its specific binding to κB sites located at various promotor regions, induces the transcription of respective proinflammatory proteins. Adapted from Barnes PJ, Karin M[54].

Phosphorylation of serine residues S536 and S468 on the transactivation domain (TAD) of p65 allow nuclear translocation of NF-κB[59]. Approximately 30 mins downstream of TNFR1 marks NF-κB to DNA binding, where TNF-α target genes VCAM-1, ICAM-1, CCL2 and IL-8 are induced[53]. (Figure 5)

Termination of the canonical NF-κB activation relies on receptor downregulation and a negative feedback loop[58]. Lysosomal degradation of TNF-α:TNFR1 complexes is responsible for decreasing cell membrane receptor density[57]. A negative feedback loop is initiated by NF-κB induced IκBα transcription and resynthesis[58]. This mechanism limits NF-κB response but does not terminate its transcriptional activity. NF-κB activity is affected by co-activators and co-repressors like HDACs that displace co-activators[60]. Several studies reveal how HDACs can alter NF-κB transcriptional activity if TNF-α-stimulated cells undergo unspecific HDAC inhibition with TSA[61]. COMMD family of proteins is an important regulator of p65-mediated transcriptional activity. COMMD1 recruits SOCS1-ECS-complex to ubiquinate p65 for proteasomal degradation[53]. This process is initiated by phosphorylation of S468 on the TAD of p65 by IKKβ and others[62]. However, it is is still unclear how COMMD1-dependent termination of p65 is affected as s468 phosphorylation also potentiates p65 binding to co-activator CBP/p300, which results in increased p65 transcriptional activity[59].

1.4 TNF-α Induces MAP Kinase Signaling

Mitogen-activated protein (MAP) kinase exists in many isoforms[64]. All 3 major groups of MAP kinase signaling can be induced by TNF-α: the extracellular signal-regulated kinases (ERK), the p38 MAP kinases and the cJun NH2-terminal kinases (JNK)[65,66]. To initiate each signaling cascade, sequentially acting protein kinases including MAP kinase kinase (MAP2K or MKK), MKK kinase (MAP3K or MKKK) and others are required. Correct corresponding phosphorylation of downstream transcription factors, mRNA interacting proteins and other substrates is critical for the specific cellular response to a stimulus like TNF-α[66].

Tumor progression Locus 2 (TPL2) guards TNF-mediated activation of ERK1 and ERK2 by MAP2K isoforms[67]. IKKβ has an important function in the canonical NF-κB pathway where it releases p65:p50 complex from IκB-α. While here, IKKβ is responsible for releasing and activation of TPL2 from TPL2:ABIN:p105 complex in resting cells[68,69].

Looking at JNK and p38 signaling more closely, these are collectively classified as stress-activated MAP kinase pathways[64,70]. A wide range of different MAP kinase isoforms are required for JNK and p38 activation. Although TPL2 is primarily attributed to ERK activation, several studies report on cell-type specific role of TPL2 in TNF-α stimulated activation of stress-activated MAP kinases. Moreover, ERK1 and ERK2 play an important role in regulating cytokine production by both transcriptional and post-transcriptional mechanisms[68]. p38 MAP kinase was shown to upregulate NF-κB expression and possibly mark promoters for potentiated NF-κB recruitment[71]. Nevertheless, it is unclear how p38 impacts TNF-mediated cellular response, as p38 activation is also linked to reduced NF-κB activity via TAK1 downregulation[71,72].

In summary, existing evidence indicates complex co-dependent activation pathways of major MAP kinase signaling groups[73]. Similarly, activation of NF-κB and MAPK signaling pathways could be dependent on direct interaction of HDAC9 with cross-talk enzymes like IKKβ. Looking at the

molecular structure of HDACs could us better understand how they interact with other proteins and affect signaling pathways pivotal in atherosclerotic plaque formation.

1.5 Histone Deacetylases

In eukaryotic cells, DNA is mostly present as condensed chromatin[74]. These are held together by electrostatic interactions between positively charged histone proteins and the negative DNA backbone which hinder binding of transcription factors[74]. Histone acetylation is one of the posttranslational modifications which can affect these electrostatic interactions and acts as an important mechanism for transcriptional control[75]. Once an Acetyl-group attaches to one of the Lysine-rests, chromatin relaxes and makes genomic DNA accessible for transcription[74-76]. Histone deacytelases (HDACs) and histone acetyltransferases (HATs) are two families of enzymes responsible for this process and many other non-histone protein interactions in numerous molecular pathways[75,76].

In general, gene regulation plays a critical role in normal embryonic physiology and adult development[75]. However, same regulatory mechanisms can be involved in pathologic processes. In fact, recent studies reveal a growing number of diseases to be linked to abnormal gene expression controlled by HATs and HDACs[75,77]. HDACs regulate many mechanisms of cell cycle like proliferation and apoptosis[75]. A disbalance in HDAC-mediated effects was shown in prostate, breast, stomach and uterus cancers[77]. Vascular diseases caused by atherosclerosis are linked to HDAC transcription regulation mechanisms involved in inflammatory response, extracellular matrix formation and cell proliferation[78]. A recent study demonstrated various HDAC inhibitors to attenuate neointima formation in vivo[79]. In SMCs, inhibiting HDACs induces G1 cell cycle arrest and prevents proliferation[79]. Further evidence associates HDAC4 with carotid intima-media thickness, while HDAC3 is linked to endothelial cell function and survival in the aortic wall[78,80,81]. In an animal experimental stroke model, HDAC inhibition revealed reduced infarct volumes as well as ameliorated functional outcome by proposed anti-inflammatory and neuroprotective mechanisms[82].

Acetylation and deacetylation is pivotal to the etiology of many diseases[74,75]. These processes are reversible and an interesting prospect for pharmacological intervention[83,84,]. A targeted approach to selectively inhibit HDACs could be beneficial in order to better understand and control specific HDAC-mediated pathological mechanisms[83,85]. HDAC inhibitors (HDACis) like valproate and varinostate are already used to treat patients suffering from epilepsy and T-cell lymphoma[77,86,87]. However, clinically established HDACis are non-specific, while many others are currently still in preclinical development and clinical testing[88]. For example, we recently reported a selective competitive class IIa HDAC inhibitor (HDACi) TMP195 to have atheroprotective effects in mice and induce anti-inflammatory responses in human monocytes[89]. These therapeutic prospects and strong evidence in literature underline the importance of fully understanding HDAC-mediated mechanisms in stroke and cardiovascular conditions.

1.5.1 HDAC Classification

There are 18 different HDACs (Table 1.1), which belong to 4 different classes based on sequence homology and domain organization[90]. Class I HDACs are expressed ubiquitously and are found in the nucleus. In contrast, Class IIa HDAC5 and HDAC9 have tissue-preference and are predominantly

found in the heart, muscle and brain. Class IIa HDACs can bind to transcription activators and repressors. They are also able to shuttle between the nucleus and cytoplasm, have a reduced deacetylase activity but can recruit Class I HDACs to increase their enzymatic capacity.

Table 1.1: Classification of Histone Deacetylases.

Class	HDAC	Expression
Class I	1, 2, 3, 8	ubiquitous, mainly nuclear
Class IIa	4, 5, 7, 9	brain, heart, skeletal muscle
Class IIb	6, 10	cytoplasm
Class IV	11	brain, heart, kidney, testicles

;

Class III are not show in this table, as they are primarily known as sirtuins and not recognized as classical histone deacetylases.

Just as other Class I, IIb and IV enzymes, Zn^{2+} is the co-factor of HDAC9. Class III HDACs are known as sirtuins and are NAD^{+} dependent.

1.5.2 HDAC9

HDAC9 is mainly expressed in the heart, brain and skeletal muscle tissues[90]. Atherosclerosis is the underlying cause of LVS, CAD and MI. Epigenetics and acetylation states at gene promoters play a critical role in atherosclerosis[22,23]. Risk allele at HDAC9 region is strongly associated with these cardiovascular diseases[18]. In fact, patients with SNP rs2107595 showed elevated HDAC9 mRNA expression and had increased intima-media thickness in carotid arteries and the aorta[20]. Concurrently, HDAC9 deficiency reduced overall plaque size and necrotic core formation in mouse atherosclerosis models[21]. Cell differentiation, proliferation, glucose, lipid metabolism and angiogenesis are key processes in vascular inflammation regulated by HDAC9[91-93].

In several autoimmune disease models, HDAC9 deficiency caused anti-inflammatory effects in mice by FoxP3-mediated suppression of Tregs in the adaptive immune system[94]. More recently, HDAC9 was found to play an important role in antiviral innate immunity, where it enhanced TANK-binding-kinase 1 (TBK1) activity by Lys461 deacetylation[95]. Finally, siRNA-mediated HDAC9 depletion suppressed oxLDL-induced proinflammatory expression of TNF-α[93]. These studies suggest that HDAC9 could similarly control other non-histone protein interactions and regulate transcriptional activity of proinflammatory genes in other cell types. However, limited data is available on HDAC9-mediated mechanisms in inflammatory processes responsible for atherosclerosis. In line with this evidence, this thesis focused on investigating proatherogenic processes of HDAC9 in endothelial and smooth muscle cells.

1.6 Mouse Model of Atherosclerosis

Mouse serves as the most commonly used laboratory model for atherosclerosis[96]. To ensure accelerated atherogenesis, deletion of the apolipoprotein E (*ApoE*) gene is the go-to method[97]. Dietary alterations were made and mice were fed a high-cholesterol western-type diet[98]. Influencing both of these factors facilitated plaque formation and highly comparable lesions could be observed within just weeks[96]. Their formation in mouse models was primarily in the aortic root and the aortic arch. Human lesions usually develop in the carotid, coronary and peripheral arteries. Despite these differences, plaque development and type is highly comparable in both species. In addition, possibility of further genetic manipulation, low facility costs and quicker breeding times prove the mouse to be a superior choice in atherosclerotic research.

1.7 Aims of the Study

Our group previously reported that *Hdac9* deficiency attenuates atherosclerosis in *Apoe*-deficient mice[21]. However, mechanisms contributing to the pro-atherogenic effect of HDAC9 and the functional role of HDAC9 in neointima formation after arterial injury are unexplored. The ubiquitous expression of HDAC9 in endothelial and smooth muscle cells warrants studying the role of individual cell types in HDAC9-mediated atherogenesis[90]. Chemokines and adhesion molecules govern atherosclerotic plaque development[32]. Production of these molecules by resident vascular cells plays a major role in leukocyte recruitment to the lesion site[29].

Therefore, the first aim of this study was to investigate HDAC9-mediated effects of proatherogenic molecules in two important resident vascular cells. In particular, we planned to examine the levels of VCAM-1, ICAM-1, MCP-1/CCL2 and IL-8 in HDAC9-deficient ECs and SMCs stimulated by TNF-α. Secondly, this study aimed to consolidate our *in vitro* findings by measuring the production of the same chemokines and adhesion molecules in atherosclerosis-prone *Apoe*$^{-/-}$ mice with *Hdac9* deficiency.

Thirdly, changes to SMC proliferation affected by reduced HDAC9 expression were to be analyzed. Finally, we aimed to link HDAC9 as mechanistic mediator in a signaling pathway responsible for the altered expression of proatherogenic molecules.

2. Methods

2.1 Equipment

15 ml falcons	VWR
24-well cell culture dishes	BD Falcon
50 ml falcons	BD Falcon
6-well cell culture dishes	Omnilab
96-well microplates PS, F-bottom	Greiner bio-one
Autoclave VX 150, DX 65	Systec
Biosphere filtertips, extralong (200 µl; 1250 µl)	Sargtest
Canulas No. 14 BD MicrolanceTM 3, 23G	BD Medical
Canulas No. 18 BD MicrolanceTM 3, 25G	BD Medical
Cell scrapers	BD Bioscience
Cell strainers, 40 µm	BD Falcon
Centrifuge Avanti J-26 XP with swinging rotor JS 7.5	Beckmann Coulter
Clean bench HeraSafe KS18	Heraeus
CO2 incubator HeraCell	Heraeus
Cooling centrifuge Heraeus Megafuge 16R	Thermo Scientific
Centrifuge 5417R, 5415D	Eppendorf
Cover slides 22x50 mm #1	Menzel Glas
Disposable cryotubes, 1.8 ml	Nunc
Filter tips 10 µl E long	Peqlab
Filter tips 10 µl G short	Peqlab

Forceps, scissors	F.S.T.
Freezer -80 C Hera Freeze Top	Thermo Scientific
Incubation shaking cabinet Certomat BS-1	Sartorius
Liquid nitrogen tank Cryoplus 2	Thermo Scientific
Magnetic stirrer KMO 2 basic	IKA
Microscope Axiovert 200M; camera AxioCam MRm Microscope slides superfrost Plus	Zeiss
Microscope Wilovert S	Menzel Glas
Microwave	Hund Wetzlar
Needles with cannula (0,33x12 mm, Myjector U40) PCR machine PTC-200	Siemens
pH-electrode	Terumo
pH-meter Lab 850	MJ Research
Pipetor Pipetboy	Schott Instruments
Power Supply Power Pac 200	Schott Instruments
Power Supply Power Pac 300	Integra
Power Supply Power Pac HC	Bio-Rad
Protein LoBind tubes 1.5 ml	Eppendorf
Rocking shaker ST5 CAT	Neolab
Safe lock tubes (0.5 ml; 1.5 ml; 2.0 ml)	Eppendorf
SafeGuard filter tips (20 µl; 200 µl; 1000 µl)	Peqlab
Scale CS Series, 200 g	Ohaus
Shaker ST 5 CAT	Neolab
Sterile disposable pipettes (2 ml; 5 ml; 10 ml; 25 ml)	Sarstedt

Syringe BD DiscarditTM II (5 ml; 10 ml)	BD Biosciences
Syringe Inject®-F Luer Duo (1 ml)	B. Braun
Thermo shaker Thriller	Peqlab
TipOne tips (10 µl; 200 µl; 1000 µl)	StarLab
Tissue culture flasks T25	Corning
Tissue culture flasks T80	Nunc
Tissue grinder, Type Potter-Elvehjem, smooth pestle	Wheaton
Vortex genie 2	Scientific Industries
Water bath 1005	GFL
Water purification system Mili-Q (Q-POD)	Milipore

2.2 Chemicals

2-Mercaptoethanol (β-ME) ≥ 99,0 %	Sigma
Acetone	Merck
Acrylamide (Ultra Pure Proto Gel 30 %)	National diagnostics
Agar	Invitrogen
Agarose peqGOLD Universal	Peqlab
Aluminium sulfate hydrate	Sigma
Ammonium persulfate (APS)	Sigma
Ampicillin	Sigma
Boric acid (H3BO3)	Sigma
Bovine serum albumin (BSA)	Sigma
Bromophenol blue	Sigma
Coomassie brilliant blue G250	Fluka
Cresyl violet acetate	Sigma
Dimethyl sulfoxide (DMSO)	Sigma
Disodium phosphate (Na2HPO4)	Merck
Dithiothreitol (DTT)	Sigma
Ethanol 70 %	Roth
Ethanol 96 %	Roth
Ethanol absolute, for analysis	Merck
Ethylenediaminetetraacetic acid (EDTA)	Roth
Eukitt®	Fluka
Glycerol ≥ 99.5 %	Roth

Glycine	Sigma
Heparin-Natrium-5000	Ratiopharm
HEPES	Roth
Hydrogen chloride (HCl)	Roth
Ketamine hydrochloride Ketavet® 100 mg/ml	Pfizer
Lithium carbonate (Li2CO3)	Roth
Luxol® fast blue	Merck
Methanol ≥99 %	Roth
Monopotassium phosphate (KH2PO4)	Merck
NP-40	Fluka
Orange G	Sigma
Paraformaldehyde (PFA) 4 % in PBS 7.4	Morphisto
Peptone from casein	Serva
Phosphoric acid	Sigma
Protease inhibitor (cOmplete, Mini, EDTA-free cocktail tablets)	Roche
Select agar	Invitrogen
Skim milk powder	Fluka
Sodium bicarbonate (NaHCO3)	Sigma
Sodium chloride (NaCl)	Roth
Sodium chloride (NaCl) 0.9 %	B. Braun
Sodium deoxycholate	Sigma
Sodium dodecyl sulphate (SDS) Pellets	Serva
Sodium fluoride (NaF)	Sigma

Sodium hydroxide (NaOH)	Roth
Sodium orthovanadate (Na2VO4)	Sigma
Tetramethylethylenediamine (TEMED)	Roth
Tris(hydroxymethyl)aminomethane (Tris) HCl	Roth
Tris, Trizma® base	Sigma
Triton X-100	Sigma
Tween-20	Roth
Xylazin 2 %	Albrecht
Xylene cyanole	ICN
Yeast extract	Roth

2.3 DNA Methods

2.3.1 Bacteria Transformation

An aliquot of competent HD5α bacteria was thawed on ice and 15 µl of bacteria cells was instantly mixed in an Eppendorf tube with 2 µl NF-κB/β-Galactosidase at 4°C and incubated for 30 mins on ice. To facilitate DNA uptake, a heat shock was performed in a water bath at 42°C for 30 s. Next, 250 µl of LB-medium were added to the mixture and incubated on a shaker at 37°C for 1 h. 250 µl of the contents were then evenly spread out onto an LB agar plate with Ampicillin and placed into an incubator overnight at 37°C.

2.3.2 Bacteria Conservation

To store the transformed cells, following overnight incubation 500 µl of HD5α bacteria were mixed in LB culture in 500 µl 85% sterile Glycerol and kept at -80°C.

2.3.3 Maxi-Preparation

To achieve higher amount of highly concentrated DNA, 150 µl of LB-Medium was mixed with Ampicillin (1:1000) in conical flasks. 2-3 colonies from each agar plate or 500 µl of conserved bacteria were isolated into each conical flask and incubated on a shaker at 37°C, 220 Upm for 16-20 h.

2.3.4 Plasmid Preparation

To prepare plasmids, Qiagen Plasmid MIDI Kit was used. Overnight-grown bacteria were centrifuged at 4°C, 11,500 rpm for 20 mins. The supernatant was disposed and the pellet was resuspended in 4 ml of Buffer 1. Cells were then lysed with 4 ml of Buffer 2 and neutralized with 4 ml of Buffer 3. The lysate was then cooled on ice for 15 mins, distributed equally into Eppendorf tubes and centrifuged at 4°C, 12,000 rpm for 45 mins. Next, isolated supernatant was centrifuged at

4°C, 17,000 rpm for 20 mins and Qiagen Tips were equilibrated with 4 ml QBT Buffer. After centrifugation, the supernatant was placed onto equilibrated Qiagen Tip for complete flow-through. Qiagen Tip was washed twice with 10 ml QC-Puffer. DNA was elated with 5 ml of QF Buffer and precipitated using 70% isopropanol at -20°C for 5 mins. The contents were centrifuged at 4°C, 15,000G at 4°C, supernatant was disposed and the pellet was washed with 70% Ethanol and air-dried for 5 mins. Ready plasmids were stored at -20°C.

2.3.5 NF-κB Luciferase Reporter Assay

The NF-κB luciferase reporter construct pIgk3ConAlux (kind donation by Dr. Mathias Baens, University of Leuven, Belgium) and the β-galactosidase construct pEQ176 (kind donation by Dr. Bernhard Lüscher, RWTH Aachen University, Germany), 1 µg each, were co-transfected with siRNA duplexes, into HUVECS. After 48 h of recuperation, cells were stimulated with TNF-α (20 ng/ml) for different time points and harvested on ice, using reporter lysis buffer (Promega). To investigate the effect of HDAC9 on NF-κB activity, bioluminescence was measure via luciferase reporter assay. Transcribed regulatory elements control the expression of the luciferase gene (Firefly luciferase gene of *Photinus pyralis*), which after being transcribed into the enzyme luciferase would react with the added substrate. Measured light intensity correlated with NF-κB activity. HUVECs were assayed for luciferase and β-galactosidase using Bright-Glo Luciferase Assay System and β-Galactosidase Enzyme Assay System (Promega). Absorbance measurements were performed in double repeats in a 96-well plate and quantified by a plate reader at 420 nm (BioRad). The luminescence of Luciferase was measured and quantified by a luminometer (Glo-Multi Detection System, Promega). Luciferase values were normalized to β-galactosidase values to correct for difference in transfection efficiency (plotted as luciferase/β-galactosidase activity).

2.3.6 RNA Isolation

To isolate RNA from cultivated HUVECs and HAoSMCs the RNeasy Mini KIt (Qiagen) was used according to manufacturer's instructions. Treatment of samples with DNase prevented contamination of genomic DNA. The RNase-free DNase Set (Qiagen) was used according to manufacturer's instructions. Isolated RNA was elated in 30 µl RNase free H_2O. Concentrations were measured photometrically using Nanodrop.

2.3.7 cDNA-Synthesis

To synthesize cDNA from isolated RNA, Omniscript RT Kit (Qiagen) was used according to manufacturer's protocol. 60 ng to 1 µg of total RNA and dT Primers (Metabion) were added for the reaction. Reagents were incubated at 37°C for 1h.

2.3.8 Quantitative real-time PCR

Primer Sequences used for RT-PCR:

Gene (human)	Primer Sequence
GAPDH for	5'- GCCTCAAGATCATCAGC-3'
GAPDH rev	5'-ACCACTGACACGTTGGC-3'
CCL2 for	5'-GATCTCAGTGCAGAGGCTCG-3'
CCL2 rev	5'- TGCTTGTCCAGGTGGTCCAT-3'
VCAM-1 for	5'-TGTGCCCACAGTAAGGCAGGC-3'
VCAM-1 rev	5'- AGCTGGTAGACCCTCGCTGGA-3'
ICAM-1 for	5'-GCTCCTGCCTGGGAACAACCG-3'
ICAM-1 rev	5'-GGGGAGGGGTGCCAGTTCCA-3'
IL-8 for	5'-CTGGCCGTGGCTCTCTTG-3'
IL-8 rev	5'-CCTTGGCAAAACTGCACCTT-3'

The quantitate analysis in Real-Time PCR (q-PCR) was performed by mixing cDNA 1:9. All experiments were performed, using Brilliant II SYBR Green PCR Master Mix (Agilent Technologies) in a Light Cycler 480 (ROCHE Diagnostics). GAPDH was used as the house-keeping gene. Measurements were carried out in triplicates. $2^{-\Delta\Delta Ct}$ method was used to calculate relative expression changes: $\Delta\Delta Ct=\Delta C_{t,\ target}- \Delta C_{t,\ calibrator}$; $\Delta CT=C_{t,\ target\ gene}-C_{t,\ house\text{-}keeping\ gene}$

2.4 Protein Methods

Primary and Secondary Antibodies

1x TBST:

150 mM NaCl, 0.2 % Tween-20, 10 mM Trizma® base, pH 8.0

All the primary and secondary antibodies listed in Table 1 below were used for western blotting. The secondary antibody was conjugated with horseradish peroxidase (HRP). All antibodies were used an appropriate solution mixed in 1% or 3% BSA in 1xTBST.

Antibodies for Western Blot:

Company Name	Product Name	Dilution	Catalog No.
Santa Cruz	Anti-VCAM1	1:500	sc-8304
Santa Cruz	Anti-ICAM1	1:500	sc-8439
Cell Signaling	Anti-IκBα	1:1000	#9242
Cell Signaling	Anti-p-IκBα	1:1000	#9246
Santa Cruz	Anti-p65	1:500	Sc-372
Cell Signaling	Anti-p-p65 (Ser 468)	1:1000	#3039
Cell Signaling	Anti-p-p65 (Ser536)	1:1000	#3033
Cell Signaling	Anti-ICAM1	1:1000	#4915
Cell Signaling	Anti-IKK1/2	1:500	#2687
Cell Signaling	Anti-p-IKK2	1:500	#2697
Sigma Aldrich	Anti-β-Actin	1:5000	A2066
Sigma Aldrich	Anti-Tubulin	1:5000	T5293
Abcam	Anti-Lamin B1	1:5000	Ab16048
Santa Cruz	Anti-ERK	1:500	sc-271269
Santa Cruz	Anti-p-ERK	1:500	sc-73831
Cell Signaling	Anti-p38	1:500	#9212
Cell Signaling	Anti-p-p38	1:500	#9211
Dako	Anti-rabbit IgG HRP	1:10000	P0448
Dako	Anti-mouse IgG HRP	1:10000	P0447
Invitrogen	Anti-IgG	1:200	A-11008
Abcam	Anti-Cyclin D_1	1:200	Ab1663

2.4.1 Protein Concentration Measurement

To determine protein concentrations, the BCA protein assay kit from Peers (Rockford, USA) was used. Its standard curve was plotted using BSA TNT-Lysis buffer in varying concentrations (0 to 2 mg). The BCA protein assay allows specific detection of peptide bonds. Cu^{2+} ions were reduced to Cu^{+} ions in alkaline conditions. These in turn bond with 2 BCA molecules (Bichinolin-4-Carbonic acid) to produce a violet solution with a specific absorption of 562 nm. 10 µl of Lysate/protein standard and 200 µl of reagents A and B were pipetted into a 96 well micro-pipetting plate, making sure no cell sample has a time advantage over the other. After a 20 mins incubation at 37°C absorptions and concentrations were determined using an ELISA plate reader. The lysate was then diluted using 1x NuPAGE-LDS sample buffer (Invitrogen) containing 1 mmol/l DTT (Sigma Aldrich) for all samples to have equal concentrations.

2.4.2 SDS-PAGE

For all the Polyacrylamide-Gels for Gel-Electrophoresis, a standard produced Tris-Glycerin-Gel was used, as described below:

	10% Separating Gel	**Stacking Gel**
4x Lower Tris	1.5 ml	-
4x Upper Tris	-	556 µl
H_2O DL	2.44 ml	1.47 ml
Acrylamide	2 ml	0.276 ml
TEMED	5 µl	2.3 µl
APS (10%)	50 µl	23 µl

For total cell lysates, cells were washed with 1% cold PBS and Lysate with 1xNuPAGE-LDS-sample buffer (Invitrogen) containing 1 mmol/l DTT (Sigma Aldrich). Protease and phosphatase inhibitors (ROCHE) were added to all buffers. The solution was cooked in 95°C for 5 mins and centrifuged at 10,000 rpm. The electrophoresis was carried out at 120 V for upper gel and 150 V for lower gel. The time for completion varied between 1 to 2 h and was ended once the bottom edge of the lower gel was reached in the separation. 6-8 µl of BioRAD Precision Plus Protein Standard was used as a marker.

2.4.3 Western Blot

Blotting buffer:

192 mM glycine, 20 % methanol, 25 mM Trizma® base, pH 8.3

1x TBST

150 mM NaCl, 0.2 % Tween-20, 10 mM Trizma® base, pH 8.0

Blocking solution:

1 % BSA in 1x TBST buffer

The preparation for blotting involved: activating the PVDF membrane (Immobilon-P Transfer Membrane, Millipore Corp., USA) in methanol for 10 s and then placing it in blotting buffer for 10 mins. The gel and the membrane were then placed between sheets of Whatman blotting paper (BioRAD laboratories, Munich), which was preliminary soaked in blotting buffer. The entire apparatus was inserted into the chamber and blotting was run at 100 V, 250 mA, 50 W for 1 h. The presence of colored marker lines verified successful protein transfer to the membrane. The membrane was then blocked in 1% BSA in 1xTBST for 1h at RT and incubated overnight at 4°C with the primary antibody mixed in appropriate buffer. After multiple washes (5 x 10 mins) in 1xTBST the membrane was incubated with an appropriate HRP-conjugated antibody, washed several times (3 x 15mins) and coated with 4 ml Immobilon Western HRP Substrate (Merch

Millipore Corp., USA). Thereafter, using Fusion Fx7, protein bands were visualized and quantified by Image 1.47v Software (Wayne Rasband).

2.4.4 ELISA

HUVEC and HAoSMC secreted levels of CCL2 and IL-8 were measured by commercially available ELISA Kits (Invitrogen) according to manufacturer's protocol. Circulating CCL2 and IL-8 levels in mouse serum were measured using a commercially available ELISA Kit according to manufacturer's protocol. Samples were either measured diluted 6-fold (HUVECs and HAoSMCs) or undiluted (blood serum). Absorbance at 562nm and 420nm was measured by Multiskan RC plate reader (Thermo/LabSystems).

2.4.5 BrdU Proliferation Assay

HAoSMCs were either transfected with SCR siRNA or HDAC9 siRNA as previously described and equally plated on a 6-well plate. 50 ng/ml of PDGF-BB were then added to each plate to stimulate SMC proliferation. Cells were then incubated for 48h and washed with 1% PBS solution.

To quantify smooth muscle cell proliferation, Roche Cell Proliferation ELISA Kit was used according to manufacturer's protocol. 5-brom-2'deoxyuridine (BrdU) acted as a pyrimidine analogon and was incorporated into newly synthesized DNA of replicated cells. The BrdU labeling solution was added to cells transfected both with control SCR siRNA as well as HDAC9 siRNA and incubated at 37°C for 2 h. Thereafter, cells were fixed and DNA was denatured using the provided FixDenat solution. Cells were then washed with 1xPBS and incubated with the anti-BrdU-POD antibody for 90 mins. Antibody conjugate was then flicked off and cells were washed 3-4 times with 1xPBS solution. Finally, the substrate was added to cells and incubated until sufficient color development. To stop the reaction, 25 µl of 1 M H_2SO_4 solution was added to each well.

Absorbance was measured at 450 nm using an ELISA plate reader. The intensity of color development was directly proportional to newly synthesized DNA.

2.4.6 Immunofluorescent Confocal Microscopy

HUVECs were transfected with HDAC9 siRNA or scrambled control RNA and stimulated for appropriate time periods with TNF-α. Cells were washed with 1xPBS and fixed with 4% PFA-PBS solution for 15 mins at RT. Ammonium Chloride was used to quench the cells for 10 mins at RT. Approximately 50,000 cells per slide with 3 slides per time point were used. Permeabilization was carried out using 0.1% Triton X-PBS for 3 mins. Between each step cells were washed 3-4 times with 1xPBS. 100 µl of 0.2% FCS, 0.2% BSA and 0.002% fish skin gelatin in 1xPBS was used to block cells for 1 h. p65 primary antibody was added in 1:100 ratio to the same solution and incubated overnight at 4°C. DAPI, Phalloidin and Alexa Fluor 488-labelled secondary antibodies were incubated for 1 h at RT. Cells were washed and sealed with a coverslip coated in fluoroscopy mounting medium (Sigma). Cell imaging was performed at the confocal microscope (LSM880, Zeiss) using the 40x oil objective.

Following antibody concentrations were used:

Company Name	**Product Name**	**Dilution**	**Catalog No.**
Molecular Probes	Anti-DAPI	1:4000	D1306
Santa Cruz	Anti-p65	1:500	Sc-372
Invitrogen	Alexa Fluor 488	1:200	A-11008
Anti-Phalloidin		1:200	

2.5 Primary Cell Culture

2.5.1 Cell Cultivation

HUVECs and HAoSMCs were purchased from PromoCell, plated on T80 flasks with vapor-permeable lids coated with 4 mg/ml Collagen G (Biochrom AG) mixed in 1% PBS solution (1:100). 15-20 ml of endothelial or smooth muscle cell medium (PromoCell) was regularly changed. Within 3-4 d 95-100% confluence was achieved and cells were separated and passaged 1:2 or 1:10, depending on desired growth rate. For experiments, cells between passages 5 and 8 were usually used.

2.5.2 Cell Lysis

Cell lysis after transfection was carried out by washing each 6-well plate with 1ml 1xPBS. 1 ml 1xNuPAGE-LDS-DTT lysis buffer was used for each well. The lysate was centrifuged (5000 rpm, 5 mins,4°C) and phosphatase and protease inhibitors (ROCHE) were added. Cell lysate was stored at -20°C and used in Protein Methods.

2.5.3 Cell Count

To determine the number of cells, a Neubauer-chamber or an automated cell counter (TC20 Automated Cell Counter, BioRad) wαs used.

Using the Neubauer-chamber: 10 µl of cell suspension was placed on a special glass microscope slide with a four-square grid, where each square had 16 smaller squares inside. Average number of counted cells was multiplied by 10^4 and the volume in the Neubauer-chamber. Final value represented number of cells per ml medium. To differentiate between dead and live cells, Tryptan-Blue was added 1:1 to cell suspension. Using automated cell counter: 10 µl of cell suspension was placed on a counting slide (BioRad) and inserted into the machine. Final value represented number

of cells per ml medium. Other options were available on the device, for example determining the cell size.

Differentiation between dead and live cells was also possible if Tryptan Blue was added, as previously explained above.

2.5.4 Cell Cryoconservation

To store cells long-term, Trypsin was used to resuspend the cells. Pellets were then stored overnight in freezing medium at -80°C in a freeze-box (M.Frosty, Nalgene). Next day, cryovials were carefully transferred into a liquid nitrogen tank. When required for experiments, cells were thawed on ice and incubated at 37°C, before being transferred into T80 flasks with fresh growth medium.

2.5.5 Cell Transfection

For cell transfection, cells were resuspended, growth medium was aspirated from flasks and cells were washed twice with 1% PBS before being lysed by 1xAccutase. Transfection with pre-designed ON-TARGETplusSMARTpool human HDAC9 siRNA or non-targeting control (Dharmacon) was conducted by electroporation using HUVEC or HAoSMC Nucleofactor Kit (Lonza) at RT. First, suspended cells were centrifuged in a Falcon tube at 1.200 rpm for 5 mins. The supernatant was aspirated and the cell pellet was resuspended in fresh growth medium at 37°C. A total lumber of live cells was determined using an automated cell counter (TC20 BioRad Automated Cell Counter) by mixing a sample of the new cell suspension with Tryptan Blue in 1:1 ratio. Next, 1 million cells were pipetted into each electroporation cuvette. Cells were electroporated using pre-set settings on the electroporation device. Once transfected, fresh growth medium was added and cells were equally plated on 6-well plates precoated with Collagen G, as mentioned in „Primary Cell Culture“. Before entering the experiment, cells were recuperated for 48-72 h. HUVECs and HAoSMCs were stimulated with 20 ng/ml human TNF-α (PeproTech) at different time points. Where necessary, supernatant was isolated to measure cytokine levels by ELISA.

2.6 Animal Experiments

2.6.1 Mouse Model

Hdac9$^{-/-}$*ApoE*$^{-/-}$ mice were generated as previously described. Mice had ad libitum access to food, water and were housed in a specific pathogen-free animal facility under a 12 h light-dark cycle. Depending on the experiment, mice were fed a high-cholesterol western-type diet or low-cholesterol chow-diet for 2 or 8 weeks. All animal experiments and data analysis were performed under blinded conditions for the genotype and were approved by the local ethics committee.

2.6.2 Tissue Harvesting

Ketamine/Xylazine anesthesia:
0.6 ml Ketamine 10 %, 0.2ml Xylazine 2 %, 0.2 ml 0.9 % NaCl solution; injection per mouse: 0.3-0.4 ml (6-8 mg/kg Xylazine, 90-120 mg/kg Ketamine)

Mice were anesthetized using ketamine-xylazine or medetomidine-midazolam-fentanyl. Blood was obtained by cardiac puncture and the arterial tree was perfused through the left ventricle with 0.9% sterile NaCl. To measure cytokine levels by ELISA, plasma was separated by centrifugation for 20 mins at 2,000 rpm, and stored at -80°C in EDTA-coated tubes. For protein analysis by western blot, entire aorta was dissected, flash-frozen and lysed in RIPA buffer containing EDTA-free phosphatase and protease inhibitors (ROCHE) by Ika T8 Ultra Turrax Tissue Homogenizer. Aorta samples were stored at -80°C.

2.7 Statistical Analysis

Statistical analysis was performed with GraphPad Prism 6 (Graph Pad Software Inc.). Data are represented as means +- s.e.m.. After testing for normality, data were analyzed by two-tailed unpaired Student's t-test or Mann-Whitney test, one-way or two-way ANOVA with Bonferonni comparison test. p-values<0.05 were considered to be statistically significant.

3 Results

3.1 Efficiency of siRNA-mediated HDAC9 Knockdown in ECs and SMCs

To investigate HDAC9-controlled inflammatory responses in resident vascular cells, expression of chemokines and adhesion molecules in primary human ECs and SMCs was examined. HUVECs and HAoSMCs were transfected with HDAC9 siRNA or scrambled control (SCR) RNA for 72 h followed by stimulation with TNF-α (20 ng/mL) for indicated time points or left untreated. The efficiency of siRNA-mediated knockdown of HDAC9 mRNA expression was 55% in HUVECs and 60% in HAoSMCs (Figure 6A,B).

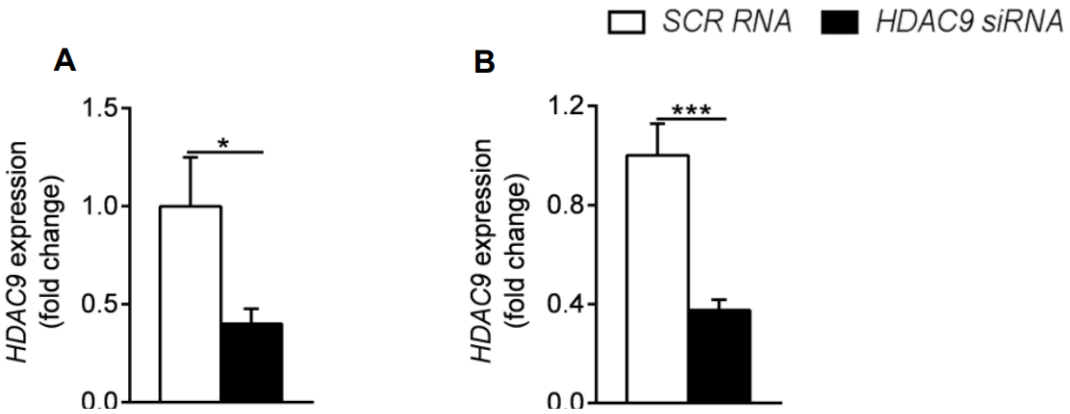

Figure 6. Efficiency of siRNA-mediated HDAC9 Knockdown in Human ECs and VSMCs. (A-B) Analysis of mRNA levels by real time-PCR. (A) HUVECs and (B) HAoSMCs were transiently transfected with HDAC9 siRNA or scrambled control (SCR) RNA for 72 h, and subsequently stimulated with TNF-α (20 ng/mL) for indicated time periods or left untreated. Quantification of HDAC9 in HUVECs and HAoSMCs. Data represent means ±SEM of 6-8 independent experiments. Unpaired t-test or Two-way ANOVA with Bonferroni post-test, as appropriate, for comparison of HDAC9 siRNA vs. SCR RNA: *, $p<0.05$; ***, $p<0.001$.

3.2 HDAC9 Promotes Expression of Chemokines and Adhesion Molecules in ECs and SMCs

HDAC9 knockdown resulted in reduced expression of IL8, CCL2, ICAM-1, and VCAM-1 in both HUVECs (Figure 7A,C) and HAoSMCs (Figure 7B,D). IL-8 expression in HUVECs (Figure 7A) was reduced by ca. 65% and by ca. 60% in VSMCs (Figure 7B). CCL2 expression showed a greater range of suppression of ca. 65-85% in both cell types upon HDAC9 knockdown and TNF-α stimulation (Figure 7A,B). Analysis of adhesion molecules at the 8h time point also revealed reduction in expression under similar conditions in both ECs and SMCs (Figure 7C,D).

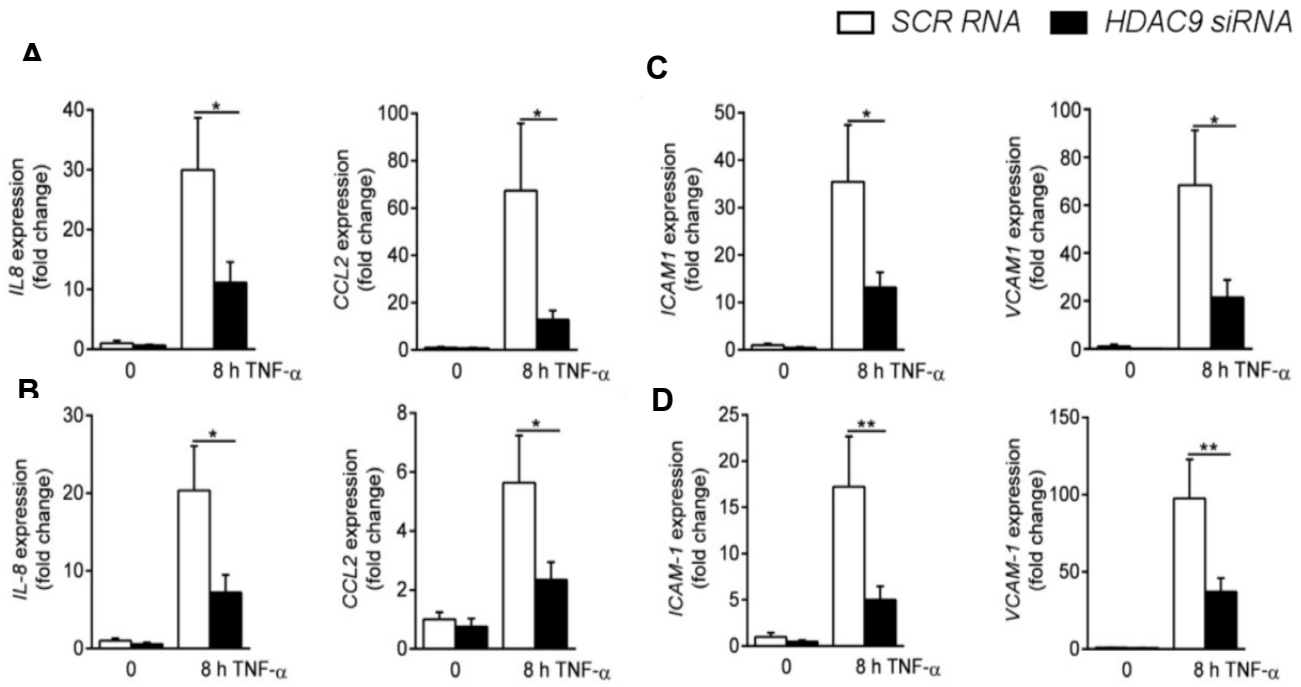

Figure 7. HDAC9 Promotes Expression of Chemokines and Adhesion Molecules in Vascular Endothelial and Smooth Muscle Cells. (A-D) Analysis of mRNA levels by real time-PCR. (A-B) HUVECs and (C-D) HAoSMCs were transiently transfected with HDAC9 siRNA or scrambled control (SCR) RNA for 72 h, and subsequently stimulated with TNF-α (20 ng/mL) for indicated time periods or left untreated. Quantification of (A) IL8, CCL2 (B) ICAM-1, VCAM-1 in HUVECs and (C) IL8, CCL2 (D) ICAM- 1, VCAM-1 in HAoSMCs. Data represent means ±SEM of 6-8 independent experiments. Two-way ANOVA with Bonferroni multiple comparison test for comparison of HDAC9 siRNA vs. SCR RNA: *, $p<0.05$; **, $p<0.01$; ***, $p<0.001$; ****, $p<0.0001$.

3.3 HDAC9 Increases Protein Levels of Chemokines and Adhesion Molecules in ECs and SMCs

Except for CCL2 levels in HAoSMCs, chemokine protein levels (Figure 8A,C) were fully concordant with mRNA expression data (Figure 8A,B), indicating that HDAC9 promotes proinflammatory responses in vascular cells. While no detectable adhesion molecules were measured in resting cells, HDAC9 knockdown and subsequent TNF-α stimulation cause endothelial ICAM-1 (Figure 8B) to be significantly lower at a later time-point (24h) , compared to ICAM-1 in HAoSMCs (16h) (Figure 8D). Similar HDAC9-mediated effect was observed with endothelial VCAM-1 (Figure 8B) compared to VCAM-1 in HAoSMCs (Figure 8D).

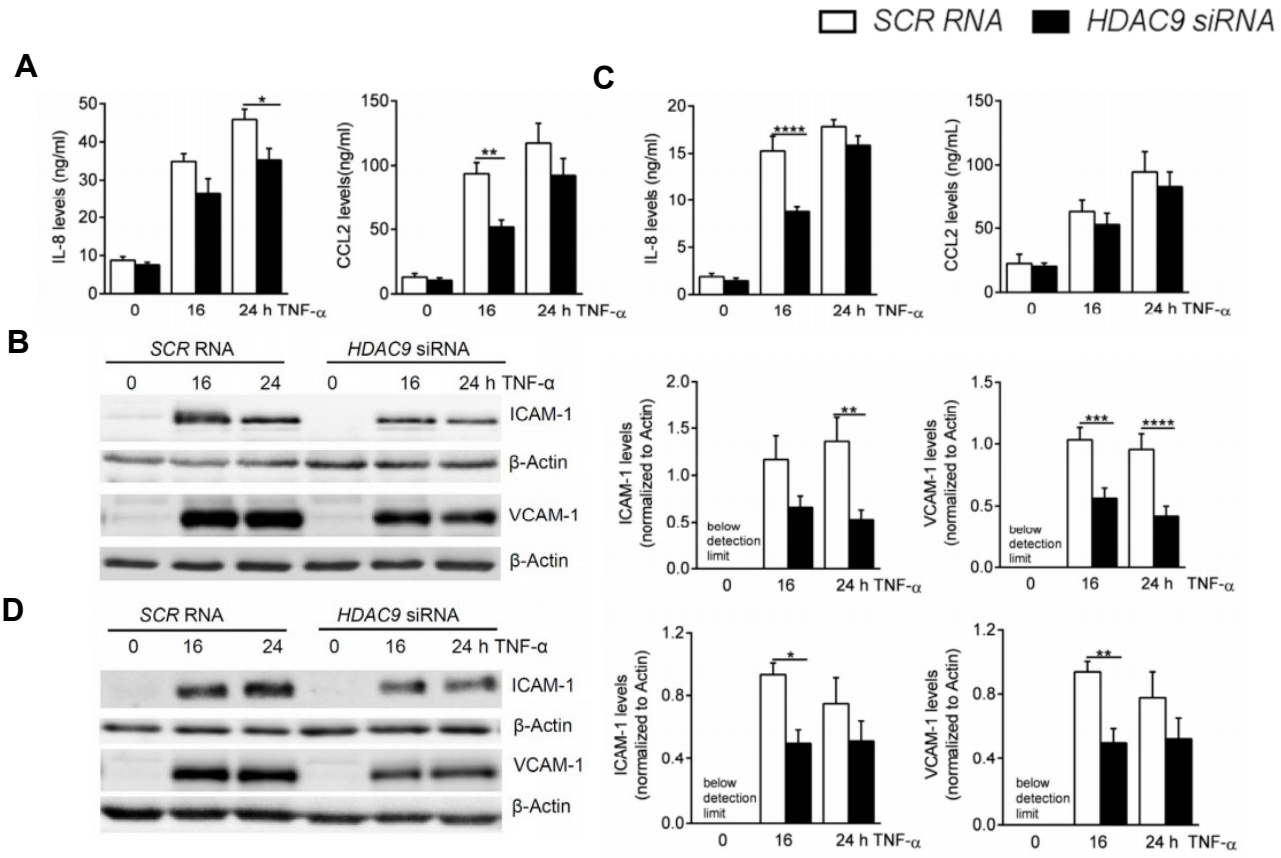

Figure 8. HDAC9 Promotes Expression of Chemokines and Adhesion Molecules in Vascular Endothelial and Smooth Muscle Cells. (A-B) HUVECs and (C-D) HAoSMCs were transiently transfected with HDAC9 siRNA or scrambled control (SCR) RNA for 72 h, and subsequently stimulated with TNF-α (20 ng/mL) for indicated time periods or left untreated. Analysis of protein levels by ELISA and western blot. IL8, CCL2 in HUVECs (A) and in HAoSMCs (C) and ICAM- 1, VCAM-1 in HUVECs (B) and in HAoSMCs (D) were quantified. Shown are representative immunoblots. Data represent means ±SEM of 6-8 independent experiments. Two-way ANOVA with Bonferroni multiple comparison test for comparison of HDAC9 siRNA vs. SCR RNA: *, $p<0.05$; **, $p<0.01$; ***, $p<0.001$; ****, $p<0.0001$.

3.4 HDAC9 Deficiency Attenuates Pro-Atherosclerotic Molecules in Atherosclerosis-prone Mice

To consolidate in vitro findings on adhesion molecule expression in vivo, Western blot analyses of whole aortas from Hdac9$^{-/-}$Apoe$^{-/-}$ and control littermate Hdac9$^{+/+}$Apoe$^{-/-}$ mice receiving Western-type diet for 2 weeks was performed. Vcam-1 levels were markedly reduced in Hdac9-deficient aortas compared to WT controls (Figure 9A). Icam-1 levels in the aorta (Figure 9A,C) and of circulating Ccl2 levels in serum were also significantly reduced (Figure 9C). The effect of Hdac9 deficiency on Vcam-1 and Icam-1 was not restricted to hyperlipidemic conditions as aortic Vcam-1 and Icam-1 levels were likewise reduced in Hdac9$^{-/-}$ mice compared to both WT controls and Apoe$^{-/-}$ mice all on chow diet (Figure 9B,D)

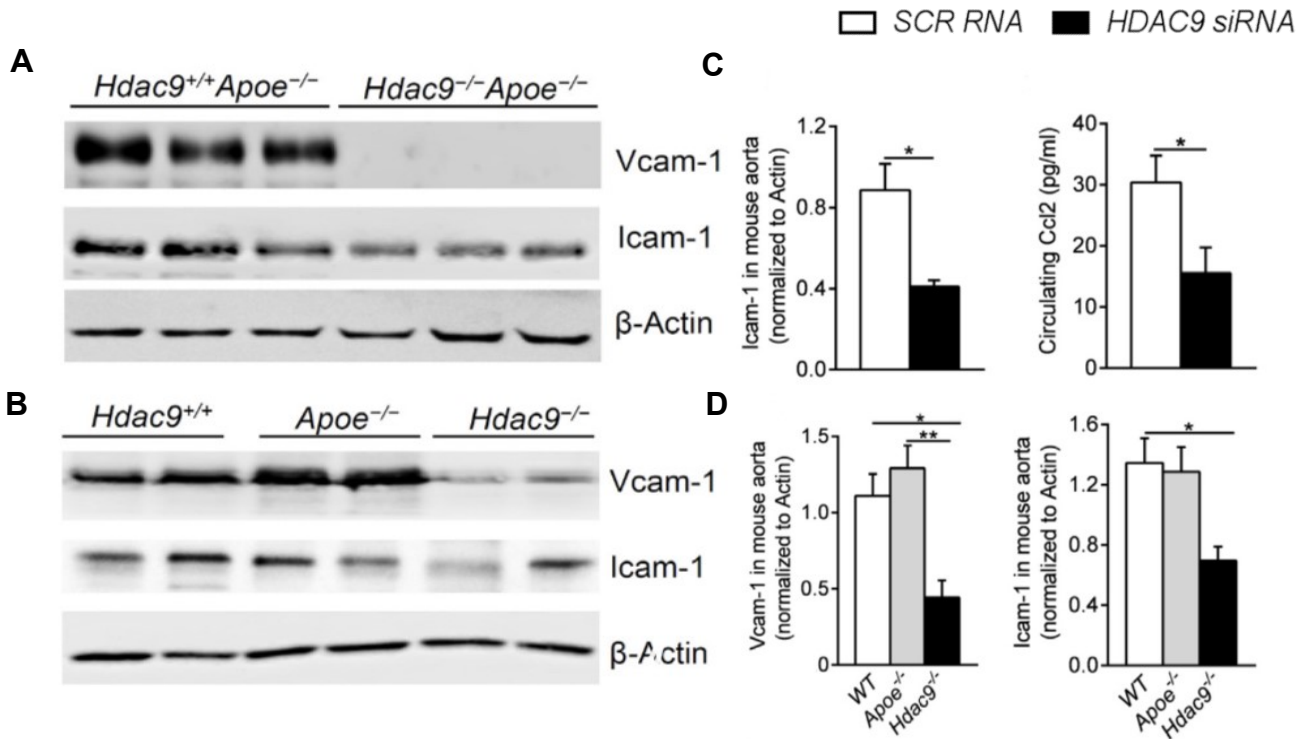

Figure 9. Hdac9 Deficiency Attenuates Secretion of Pro-Atherosclerotic Molecules in Atherosclerosis-prone Mice. (A,C) Examination of adhesion molecules and chemokines in hyperlipidemic Hdac9$^{-/-}$Apoe$^{-/-}$ and Hdac9$^{+/+}$Apoe$^{-/-}$ control littermate mice receiving western-type diet for 2 weeks. (A, B) Determination of Vcam-1 and Icam-1 in whole aortas (n = 5-7 mice per group) as well as (C) circulating Ccl2 levels in serum (n = 4-7 mice per group). (B,D) Examination of adhesion molecules in vivo in naive mice. Vcam-1 and Icam-1 were determined in whole aortas from WT, Apoe$^{-/-}$ and Hdac9$^{-/-}$ mice receiving chow diet for 9 weeks (n = 4 per group). Data represent means ±SEM. Two-way ANOVA with Bonferroni multiple comparison test, unpaired t-test or Mann-Whitney test, as appropriate, for comparison of HDAC9 siRNA vs. SCR RNA or Hdac9$^{-/-}$Apoe$^{-/-}$ vs. Hdac9$^{+/+}$Apoe$^{-/-}$ control: *, $p<0.05$; **, $p<0.01$; ***, $p<0.001$.

3.5 HDAC9 Enhances NF-κB Activity and p65 Nuclear Translocation

The observed pattern of pro-inflammatory gene expression resembles NF-κB-mediated responses in atherogenesis. Hence, effects of HDAC9 depletion on NF-κB signaling were explored. After TNF-α stimulation and siRNA-mediated HDAC9 knockdown of primary human ECs, NF-κB luciferase activity was measured and quantified. HDAC9 depletion significantly reduced NF-κB activity (Figure 10A). A clear reduction in NF-κB activity began 4h after TNF-α stimulation and the highest difference between transfected and control HUVECs was demonstrated at the 24h time-point. Western Blot analysis of p65 in nuclear and cytoplasmic fractions revealed decreased nuclear translocation of p65 (Figure 10B) compared to controls. HDAC9 deficiency gradually diminished p65 nuclear protein levels in both stimulated and unstimulated HUVECs (Figure 10C). Stimulation with TNF-α induces a proinflammatory response and higher nuclear p65 levels in control, while reducing initial p65 in the nucleus of ECs which underwent HDAC9 knockdown. Visualization of intercellular p65 via confocal microscopy (Figure 10D) concurred Western Blot findings. Reduced signal intensity of fluorescently marked p65 in the nucleus was demonstrated in HUVECs with diminished HDAC9 upon TNF-α stimulation.

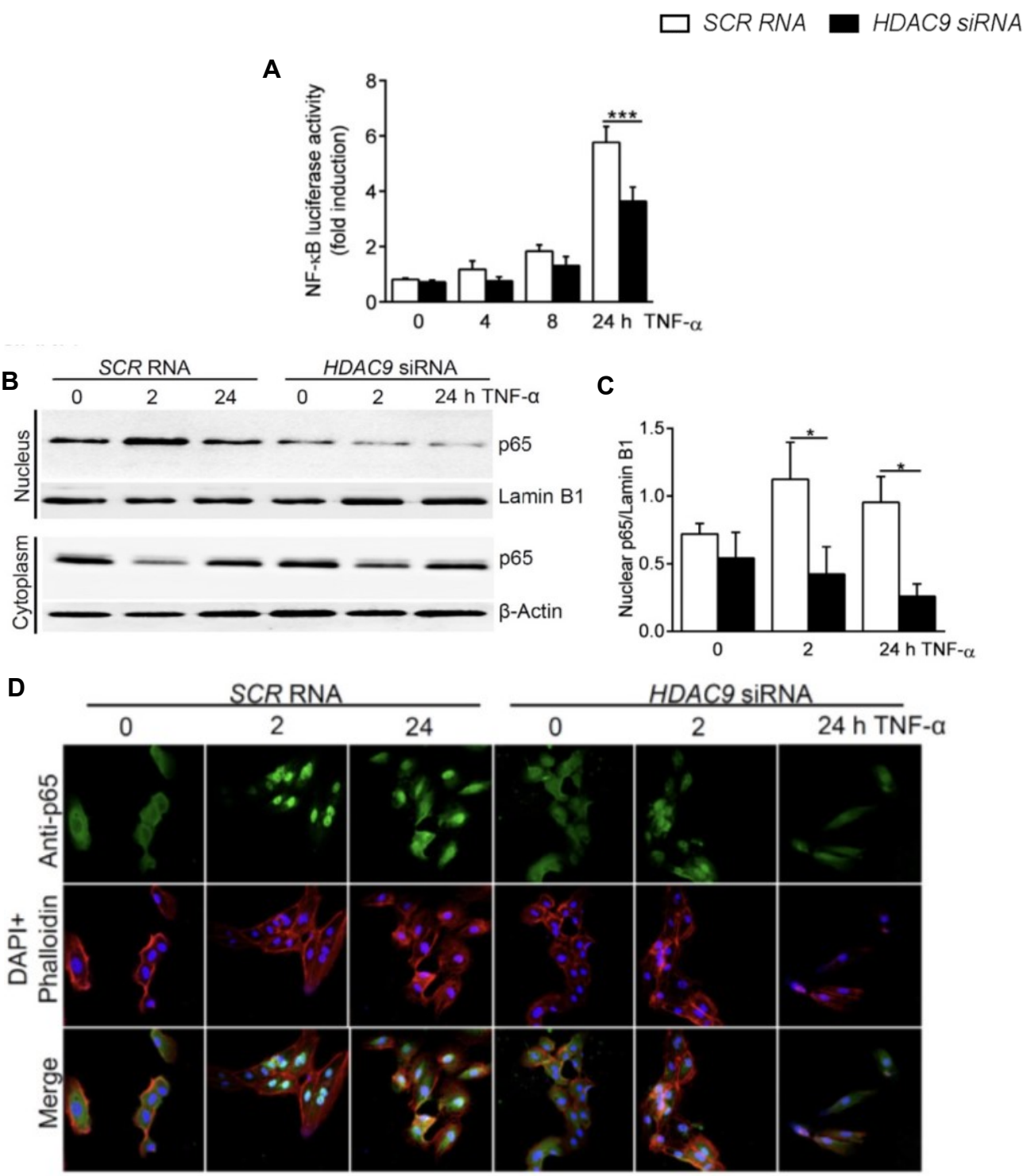

Figure 10. HDAC9 Enhances NF-κB Activity and p65 Nuclear Translocation. HUVECs were transiently transfected with HDAC9 siRNA or scrambled control (SCR) RNA for 72 h and subsequently stimulated with TNF-α (20 ng/mL) for indicated time periods or left untreated. (A) Quantification of NF-κB-dependent luciferase activity after normalization to β-galactosidase expression in HUVECs (n = 7 independent experiments). (B) Immunodetection with quantification (C) and immunofluorescence (D) of p65 in nuclear and cytoplasmic fractions and normalized to lamin B1 and β-actin respectively in HUVECs (n = 3-4 independent experiments). Data represent means ±SEM. Two-way ANOVA with Bonferroni multiple comparison test, unpaired t-test or Mann-Whitney test, as appropriate, for comparison of HDAC9 siRNA vs. SCR RNA or $Hdac9^{-/-}$ $Apoe^{-/-}$ vs. $Hdac9^{+/+}Apoe^{-/-}$ control: *, $p<0.05$; **, $p<0.01$; ***, $p<0.001$.

3.6 HDAC9 Is Required for Sustained Serine 536 and 468 Phosphorylation of p65

Since phosphorylation of Serine 536 and 436 in the transactivation domain of p65 promotes its translocation into the nucleus, the effect of HDAC9 on the phosphorylation of these serine residues was studied. siRNA-mediated knockdown of HDAC9 in HUVECs and HAoSMCs significantly reduced TNF-α-induced p65 phosphorylation at both serine residues (Figure 11A-D). In HDAC9-depleted HUVECs, largest proportion (~50%) of reduced Ser536 phosphorylation occurred at 2h (Figure 11C) following TNF-α stimulation. In HDAC9-depleted HAoSMCs, highest significant differences in Ser536 phosphorylation occurred much earlier at 5 and 15 mins after TNF-α stimulation (Figure 11D). Interestingly, Ser468 phosphorylation generally happened much sooner for both cell types. Here, peak difference between HDAC9 knockdown and controls was demonstrated 5 mins after TNF-α stimulation (Figure 11C,D).

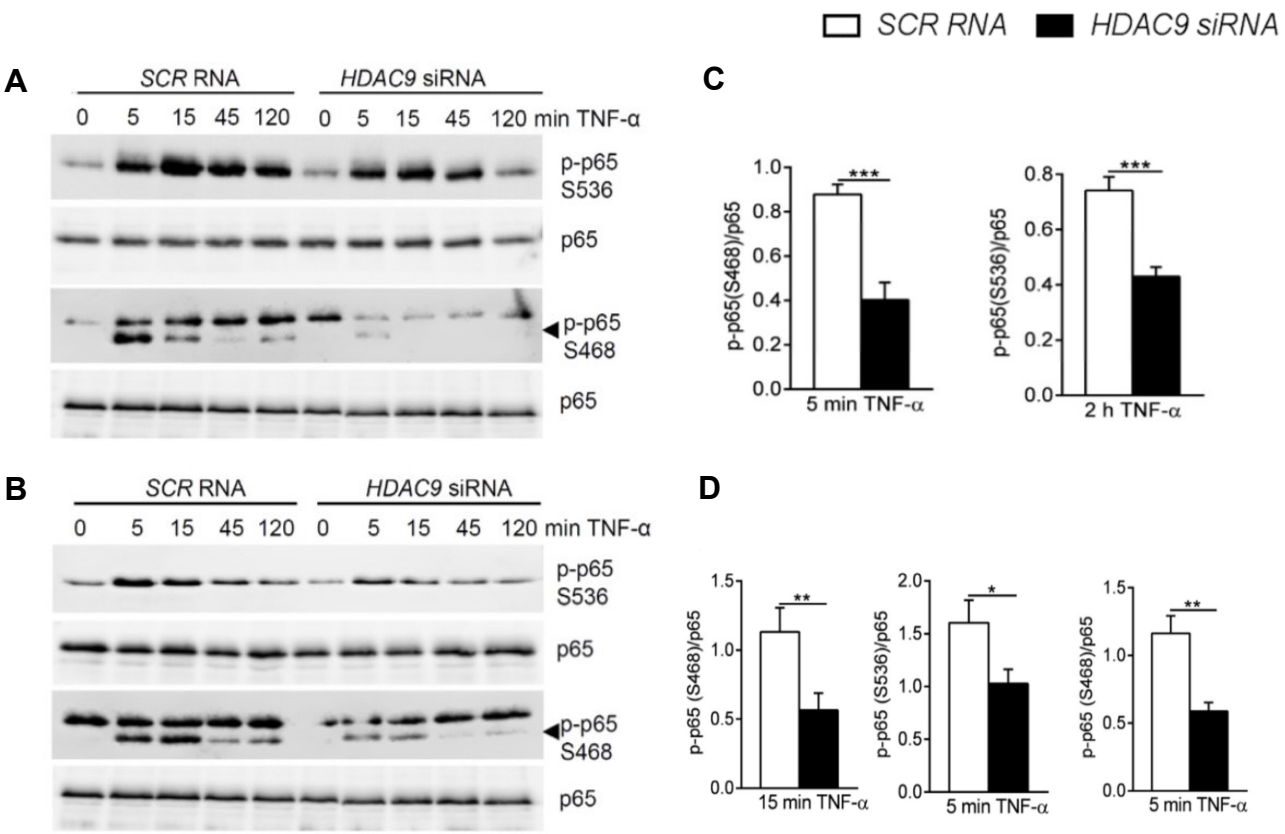

Figure 11. HDAC9 is Required for Sustained Serine 536 and 468 Phosphorylation of p65. (A,C) HUVECs and HAoSMCs (B,D) were transiently transfected with HDAC9 siRNA or scrambled control (SCR) RNA for 72 h and subsequently stimulated with TNF-α (20 ng/mL) for indicated time periods or left untreated. (A,C) Immunodetection via Western Blot of phosphorylated p65 at serine 536 and 468 normalized to total p65 in HUVECs (n = 5-8 independent experiments). (B,D) Immunodetection via Western Blot of phosphorylated p65 at serine 536 and 468 normalized to total p65 in HAoSMCs (n = 6 independent experiments). Phosphorylation of p65 at serine 536 and 468 was quantified (n=8) after normalization to total p65. Shown are representative immunoblots and densitometric analyses of time points with significant differences. Data represent means ±SEM. Two-way ANOVA with Bonferroni multiple comparison test, unpaired t-test or Mann-Whitney test, as appropriate, for comparison of HDAC9 siRNA vs. SCR RNA: *, $p<0.05$; **, $p<0.01$; ***, $p<0.001$.

3.7 HDAC9 Promotes de novo Synthesis of IκB-α

NF-κB activation is known to be accompanied by de novo synthesis of the inhibitory protein IκB-α. To further explore HDAC9 effects in NF-κB signaling, IκB-α levels were quantified upon TNF-α stimulation in HDAC9-depleted primary human ECs and VSMCs (Figure 12A-C). siRNA-mediated knockdown of HDAC9 resulted in significantly reduced TNF-α-induced de novo synthesis of IκB-α in both HUVECs and HAoSMCs at 120 mins (Figure 12B,C). Additionally, unstimulated ECs and SMCs demonstrated significantly elevated initial IκB-α levels upon HDAC9 knockdown, compared to control cells. These findings suggest that the pro-inflammatory property of HDAC9 is mediated, at least in part, through NF-κB signaling, independently of TNF-α.

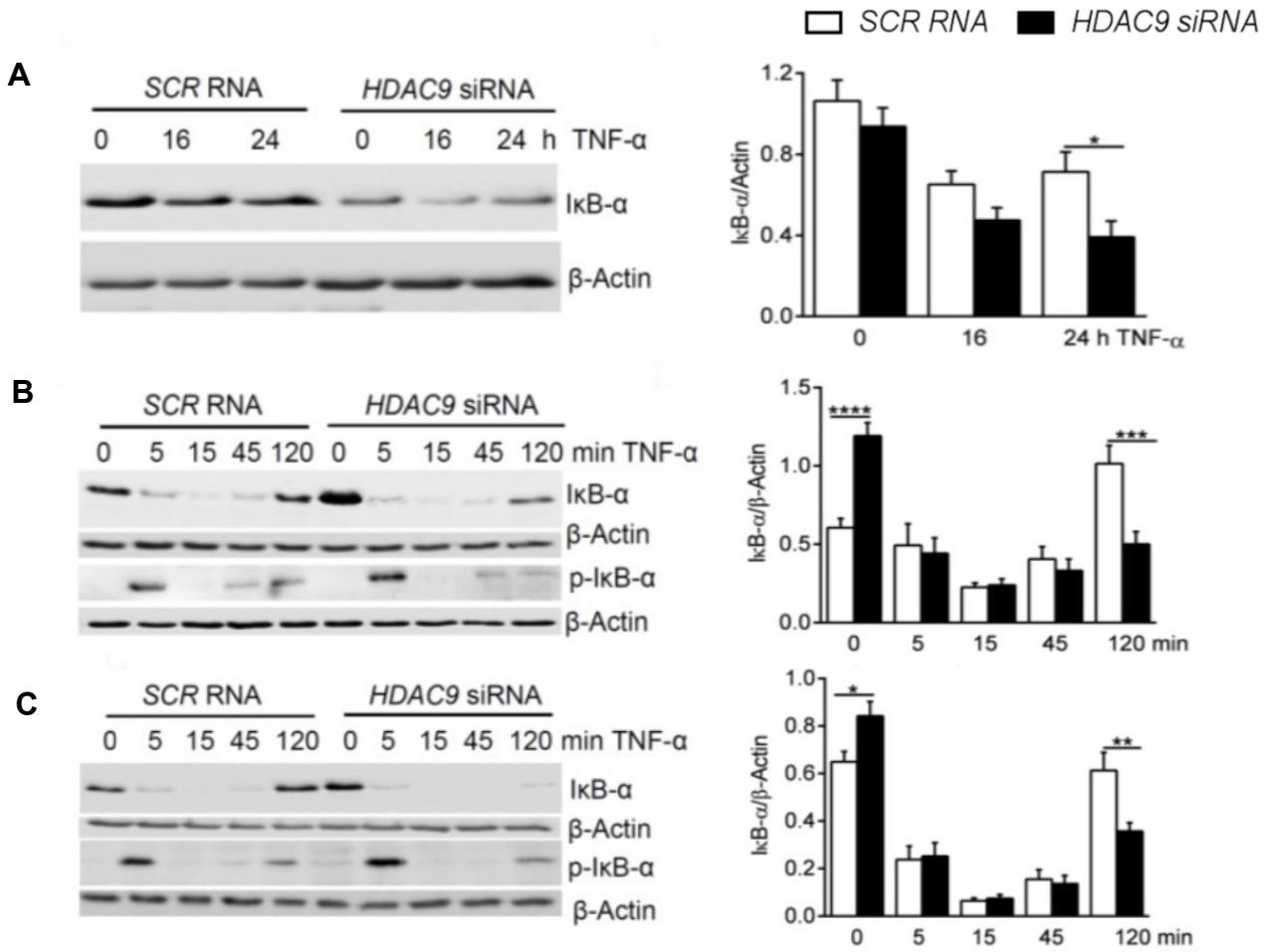

Figure 12. HDAC9 Promotes de novo Synthesis of IκB-α following Proinflammatory Stimulation. (A-B) HUVECs and (C) HAoSMCs were transiently transfected with HDAC9 siRNA or scrambled control (SCR) RNA for 72 h. Cells were stimulated with TNF-α (20 ng/mL) for indicated time periods or left untreated and prepared for protein analysis by immunoblotting. Immunodetection of IκB-α, p-IκB-α and β- Actin as loading control in HUVECs (n = 7-8 independent experiments) and in HAoSMCs (n = 6 independent experiments). Shown are representative immunoblots and densitometric analyses. Data represent means ±SEM. Two-way ANOVA with Bonferroni multiple comparison test for comparison of HDAC9 siRNA vs. SCR RNA: *, $p<0.05$; **, $p<0.01$; ***, $p<0.001$; ****, $p<0.0001$.

3.8 p38 and ERK1/2 MAPK Pathways Remain Unaffected Upon HDAC9-Knockdown

MAPK signaling is normally activated by TNF-α-induced phosphorylations of p38 and ERK1/2. To determine if siRNA-mediated HDAC9 knockdown affected MAPK pathways, primary human ECs were used to detect phosphorylated and unphosphorylated p38 and ERK1/2 (Figure 13). TNF-α induced phosphorylation of both proteins after 5 and 15 mins, however no difference between cells transfected with HDAC9-siRNA and SCR control was found (Figure 13B,C). These results indicate that HDAC9-mediated pro-inflammatory effects are probably not regulated by these MAPK pathways.

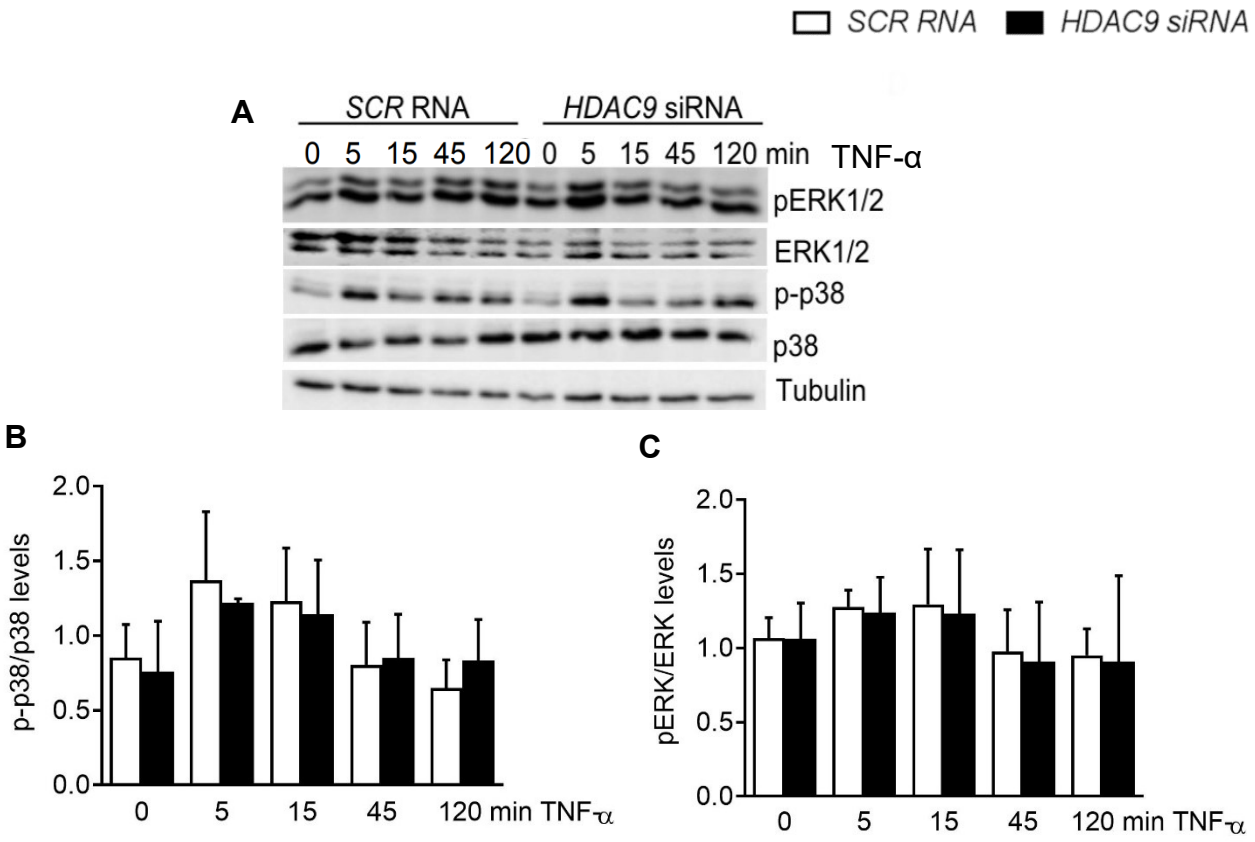

Figure 13. p38 and ERK1/2 MAPK Pathways Remain Unaffected Upon HDAC9-Knockdown. HUVECs were transiently transfected with HDAC9 siRNA or scrambled control (SCR) RNA for 72 h, and subsequently stimulated with TNF-α (20 ng/mL) for indicated time periods or left untreated. (A) Immunodetection of pERK1/2, ERK1/2, p-p38, p38, and Tubulin with specific antibodies (n = 5 independent experiments). (B,C) Quantification of pERK1/2, ERK1/2, p-p38, p38 normalized to Tubulin. Shown are representative immunoblots and densitometric analyses. Data represent means± SEM. Two-way ANOVA with Bonferroni multiple comparison test for comparison of HDAC9 siRNA vs. SCR RNA: *, $p<0.05$; **, $p<0.01$; ***, $p<0.001$.

3.9 HDAC9 Deficiency Reduces SMC Proliferation

To investigate the effects of HDAC9 on cell proliferation, HAoSMCs were transiently transfected with scrambled control or HDAC9 siRNA for 72 h (Figure 14). Following transfection, 5-brom-2'deoxyuridine (BrdU) was incorporated for 48 h under three varying conditions: (1) no serum was added, (2) serum was added and (3) serum was added with 50 ng/ml PDGF-BB (Figure 14A). Measured BrdU directly correlated with synthesized DNA of newly replicated cells. For both groups, SMC proliferation remained unaffected when serum was added. Neither was there any difference in SMC proliferation between control and cells with reduced HDAC9. However, stimulation with PDGF-BB doubled BrdU incorporation for both groups. Compared to control cells also treated with PDGF-BB, HDAC9 deficiency reduced SMC proliferation by roughly 40%. Additionally, we investigated HDAC9 effects on Cyclin D1 in SMCs stimulated with TNF-α (Figure 14B,C). Here, we found a 50% reduction in Cyclin D1 levels upon HDAC9 knockdown after 16 h and 24 h. Our findings suggest that HDAC9 deficiency reduces SMC proliferation and attenuates DNA replication in a proinflammatory milieu.

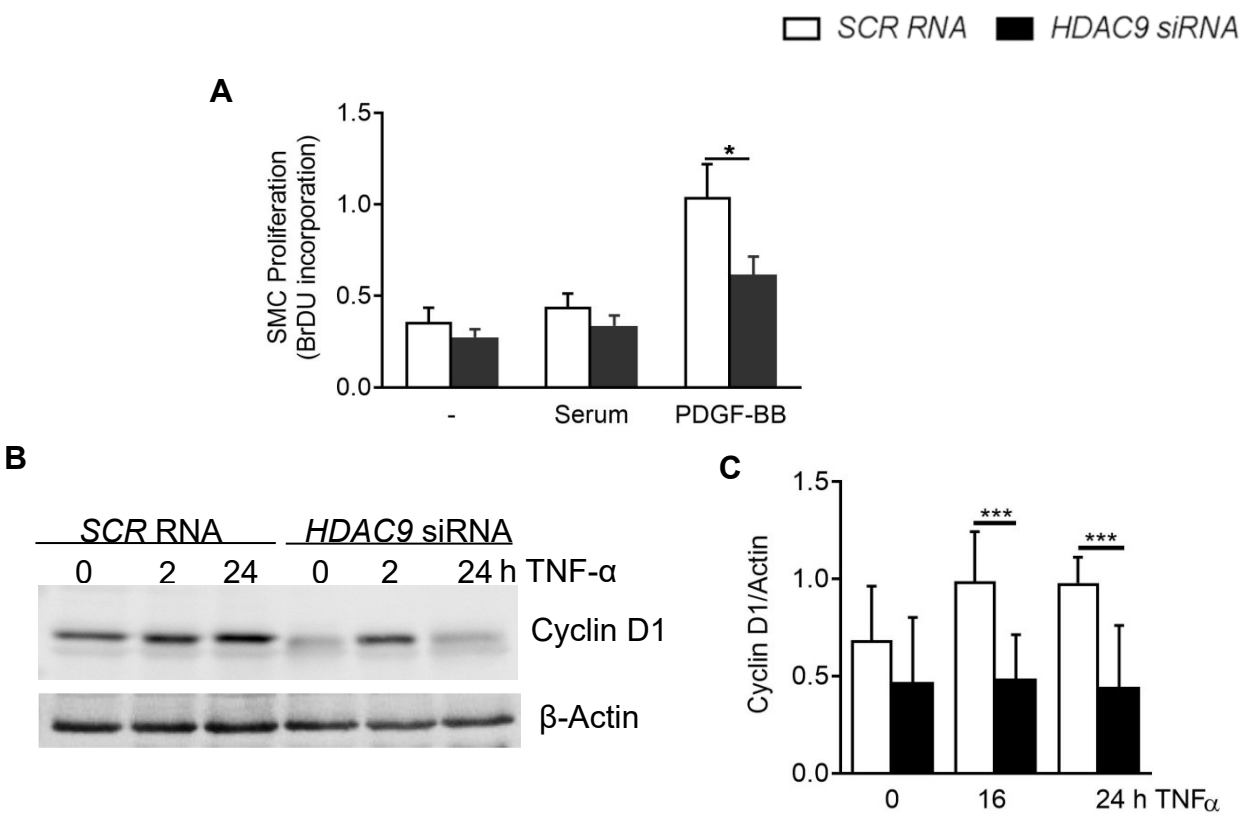

Figure 14. HDAC9-related Effects on SMC Proliferation and Cyclin D1. HAoSMCs were transiently transfected with HDAC9 siRNA or scrambled control (SCR) RNA for 72 h, and subsequently stimulated with (A) PDGF-BB for 48 h or with (B,C) TNF-α (20 ng/mL) for indicated time periods or left untreated. (A) Immunodetection of BrDU using anti-BrdU-POD antibody (n = 5 independent experiments). (B,C) Immunodetection and quantification of Cyclin D1 normalized to β-Actin. Shown are representative immunoblots and densitometric analyses. Data represent means ±SEM. Two-way ANOVA with Bonferroni multiple comparison test for comparison of HDAC9 siRNA vs. SCR RNA: *, $p<0.05$; **, $p<0.01$; ***, $p<0.001$.

4 Discussion

4.1 Summary of Results

Large vessel stroke (LVS) accounts for a quarter of all ischemic stroke and is one of leading causes of death and disability in adults worldwide[1,2]. A recent GWAS identified rs2107595 at HDAC9 as a major risk locus associated with LVS and accumulating data unequivocally demonstrated a pro-atherogenic role of HDAC9[17,19]. In fact, HDAC9-deficiency reduced atherosclerotic plaque development in $ApoE^{-/-}$ and $Ldlr^{-/-}$ mice[21,93]. HDAC9 was shown to play a major role in proinflammatory responses via direct protein interactions and gene transcriptional regulation[91,94]. However, the pathomechanism implicating HDAC9 in atherosclerotic development is still poorly understood. The results of this thesis reveal a proinflammatory role of HDAC9 in resident vascular cells both in the aorta of $ApoE^{-/-}$ mice as well as primary ECs and SMCs. Most importantly, NF-κB pathway was identified as a downstream effector of HDAC9. Our findings demonstrate vascular HDAC9 to be a key regulator of proinflammatory processes based on following evidence: HDAC9 deficiency or depletion caused: (1) reduced levels of proinflammatory molecules in ECs, VSMCs and in vivo, (2) inhibited p65 translocation into the nucleus and decreased NF-κB luciferase activity and (3) reduced VSMC proliferation. Finally, we were able to rule out MAPK signaling in inducted HDAC9-mediated responses produced in our experiments. Combined, this data suggests targeted HDAC9 inhibition as a novel precision medicine approach for restricting atherosclerotic plaque formation and improving LVS prevention.

4.2 HDAC9 Deficiency Reduced Proinflammatory Responses *in vitro* and *in vivo*

In cultured ECs and SMCs, HDAC9-knockdown attenuated TNF-α-induced production of chemokines and adhesion molecules. Our findings reveal that HDAC9 potentiates proinflammatory molecule production (ICAM-1, VCAM-1, CCL2/MCP-1, IL-8) in two important cell types involved in atherosclerosis[22]. Both mRNA expression and protein levels of molecules involved in attraction, attachment and retainment of macrophages at the atherosclerotic lesion site is diminished with lower levels of HDAC9[29]. Significant differences occurred at 16 h and/or 24 h in both ECs and SMCs. The effect at these early time points indicates the importance of HDAC9 in initiating inflammation. Existing evidence demonstrates CCL2/MCP-1 and IL-8 to induce chemotaxis and enhance monocyte tissue transmigration[37]. Hence, reduced production of these chemokines by resident vascular cells could delay attraction of circulating immune cells and decelerate their aggregation, lipid-intake and differentiation to foam cells[31,37]. Lower monocyte involvement also means reduced activation of the adaptive immune cell response at the lesion site[32,37]. As a result, directly targeting HDAC9 to inhibit production of CCL2/MCP-1 and IL-8 right at the initiation of atherosclerotic plaque development could reduce tissue lipid-retention events and subsequent endoluminal thickening of the vascular wall[28]. Previous studies of human serum demonstrated CCL2/MCP-1 to be associated with increased risk of overall stroke and IL-8 to independently predict cardiovascular events[40,43]. Thus, decreasing circulating levels of these two molecules could dramatically delay inflammation and protect vessels from atherosclerotic lesions.

Finally, *in vivo* analysis of Vcam-1 and Icam-1 in whole aortas of *ApoE*$^{-/-}$ *Hdac9*$^{-/-}$ mice concurred our results *in vitro*. Interestingly, a recent study showed HDAC3 to induce VCAM-1 production, suggesting that HDAC9 could be similarly implicated in regulating atherosclerotic molecule levels[80]. Our findings reemphasize HDAC relevance in atherogenic responses by associating HDAC9 to increased VCAM-1 expression in ECs. Moreover, additional mechanistic role of HDAC9 is unraveled, as VCAM-1 is linked to initiation and ICAM-1 to the progression of

atherosclerosis[38,39]. Thus, diminishing HDAC9 levels could reduce progression of atherosclerosis by lowering ICAM-1 levels.

4.3 HDAC9 Induces NF-κB Signaling

Our results reveal HDAC9-mediated activation of NF-κB in both ECs and SMCs. HDAC9 deficiency resulted in (1) reduced p65 phosphorylation at serine residues S536 and S468, (2) lower p65 nuclear translocation, (3) decreased *de novo* IκB-α synthesis and (4) inhibited NF-κB activation.

The barcode hypothesis defines phosphorylation of specific NF-κB subunit residues to enhance NF-κB activation[53,54]. Here, we examined phosphorylation of S536 and S468 at the TAD of p65. These serine residues promote p65 nuclear translocation and DNA binding[53,54]. In the canonical pathway, TNF-α stimulation amplifies this mechanism to induce the transcription of pro-inflammatory proteins[53]. Thus, our goal was to not only investigate HDAC9-regulated effects on the proinflammatory phenotype but to also link HDAC9 to the activation of a responsible signaling pathway.

While HDAC9 knockdown attenuated phosphorylation of p65 at S468, it is possible that decreased phosphorylation of this particular serine residue is not the driving mechanism responsible for reduced NF-κB activity[53]. In fact, previous reports suggest successful S468 phosphorylation to initiate p65 ubiquination and proteasomal degradation[53]. Therefore, better understanding of mechanisms associated with S468 phosphorylation is necessary. Additionally, further investigation of HDAC9-mediated effects on other p65 serine residues is required.

Several kinases are responsible for the phosphorylation of p65 at specific residues[53,54]. One study revealed HDAC9 to interact with TBK1, which is a known kinase of S536 but not of S468[53,95]. In contrast, IKKß is a common kinase for both of these serine residues[54]. Concurrently, our group demonstrated direct deacytelation of IKKß by HDAC9 to enhance IKKß catalytic activity[89]. (Figure 15) Previous studies already associated other HDACs with NF-κB signaling and showed Class I HDACs (HDAC 1, 2 and 3) to interact with p65 in the nucleus[56,60]. In contrast, we demonstrated HDAC9 to affect p65 in the cytoplasm and to enhance NF-κB activity in the nucleus. Additionally, we revealed HDAC9-deficiency to repress *de novo* synthesis of IκB-α, which is

responsible for forming a complex with p65:p50 heterodimer in resting cells[58]. Stimulation by TNF-α usually causes

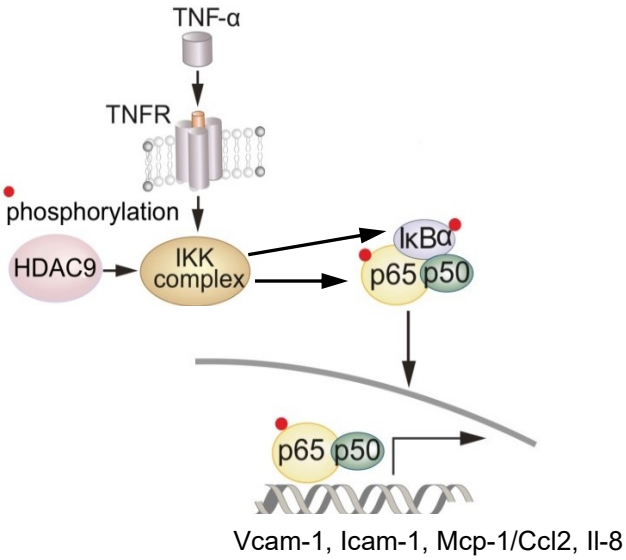

Figure 15. HDAC9 binds to IKKβ resulting in its deacetylation and activation. Schematic representation of the canonical NF-κB pathway. TNF-α binds to TNF-α receptor to result in the activation of the IKK complex, which is partially made up of IKKβ. HDAC9 directly interacts with IKKβ, resulting in increased IKKβ catalytic activity and enhanced phosphorylation of the p65 and IκBα proteins. Subsequently, freed p65:p50 translocates into the nucleus, binds to DNA and induces the transcription of proinflammatory genes Vcam-1, Icam-1, Mcp-1/Ccl2 and Il-8. Adapted from Asare et al. 2020.[89]

proteosomal degradation of IκB-α and enhanced binding of NF-κB to DNA[53]. Resynthesis of IκB-α is initiated by the same mechanism within the first 120 mins to prevent continued NF-κB-mediated inflammatory response[53,58]. Thus, lower levels of resynthesized IκB-α can be explained by reduced initial NF-κB activation and DNA binding. In fact, cells that underwent HDAC9 knockdown showed suppressed IκB-α levels 24h after TNF-α stimulation. This is in line with reduced NF-κB luciferase activity at 24h. Thus, our findings suggest HDAC9 to play a key role in both initiating and sustaining NF-κB-mediated pro-inflammatory responses.

4.4 HDAC9 Deficiency Does Not Affect MAPK Pathway

All three major groups of MAP kinase signaling including ERK, JNK and p38 MAP kinases are known to be activated by TNF-α[64-66]. The activation of ERK and p38 kinases is carried out via phosphorylation by upstream kinases[66]. These in turn activate multiple downstream mediators to activate a proinflammatory cascade responsible for the expression of proatherogenic genes[64-66].

In line with this, we decided to examine phosphorylation of ERK1/2 and p38 pathways to determine if HDAC9 plays a role in TNF-mediated MAP kinase activation. Immunodetection of phosphorylated p38 and ERK1/2 showed no difference between ECs transfected with scramble (SCR) control and HDAC9-siRNA. (Figure 13) Usually, the production of chemokines and adhesion molecules is initiated by MAPK signaling pathways. In fact, MAP kinase signaling, just like the NF-κB pathway, is crucial for a vast range of cellular functions including proliferation and differentiation[64]. Previous reports already identified several examples of complex mechanistic cross-talk between MAP kinase and NF-κB pathways[67-69]. For example, HDAC3 is part of a repressor complex that can suppress c-JUN after phosphorylation by JNK[70]. Additionally, HDAC3 was shown to be involved in the NF-κB lysine acetylation and subsequent induction of NF-κB pathway[64]. Similarly, previous reports also showed another common mediator IKKβ to be involved in both ERK and NF-κB signaling pathways[64]. Therefore, it was important to check if the effects produced by diminished HDAC9 levels are co-regulated by MAPK signaling pathways.

From results demonstrated above, we were able to conclude that HDAC9 deficiency did not attenuate the expression of VCAM-1, ICAM-1, MCP-1/CCL2 and IL-8 via ERK1/2 and p38 signaling.

4.5 HDAC9 Attenuates SMC Proliferation

As previously described in Chapter 1.2.1 more advanced atherosclerotic lesions are characterized by VSMC phenotypic switch, which marks a higher proliferation index[34]. Class II HDACs were previously shown to induce phenotypic switching in SMCs, thus promoting atherosclerotic plaque formation[78,79].

In order to investigate HDAC9-mediated effects on SMC proliferation, we examined Cyclin D_1 levels in a proinflammatory milieu. Our findings demonstrated that upon TNF-α stimulation, siRNA-mediated HDAC9-knockdown halved cyclin D1 levels. [Figure 14B,C) Furthermore, using a well-established proliferation assay, we also observed a dramatic reduction of BrdU incorporation caused by a ~50% decrease in proliferation of HDAC9 deficient SMCs. (Figure 14A)

In line with our results, reduced SMC proliferation could decrease the production of extracellular matrix proteins that lead to the formation of a thicker fibrous cap[46,51]. VSMCs play a critical role in pro-inflammatory molecule (VCAM-1, ICAM-1 and CCL2/MCP-1) production so diminishing this cell population could minimize EC activation and dysfunction, and inhibit tissue macrophage retainment[22,32]. Thus, reduced SMC proliferation caused by HDAC9-defficiency could not only attenuate atherogenesis by minimizing fibrous cap thickening but also decrease EC replication and leukocyte extravasation into the intima[34].

Furthermore, cell proliferation is marked by different stages of the cell cycle, which are controlled by interactions of cyclins (cyclins D, E and A) and cyclin-dependent kinases (cdk)[52]. In fact, S-phase is a crucial step of mitosis responsible for the synthesis of complimentary DNA strands during chromatid replication[52]. Therefore, reducing cyclin D_1 levels via HDAC9 knockdown results in less cyclinD:cdk4/6 complexes driving G1/S-phase transition[52]. This data further supports our findings of reduced SMC proliferation by measuring BrdU incorporation in newly synthesized DNA. (Figure 14A)

We are able to postulate that HDAC9-mediated reduction of SMC proliferation could be associated with decreased atherosclerotic development and is responsibly for reduced lesion size reported in

ApoE$^{-/-}$Hdac9$^{-/-}$ mice[21]. Non-specific HDACis TSA and butyrate were previously demonstrated to both up- and downregulate Cyclin D_1, pointing to possibly differing roles of HDACs in SMC proliferation[34]. However, the exact roles of individual HDACs remain poorly explained to fully understand these effects. Our novel findings, demonstrate HDAC9 to regulate SMC proliferation and support the potential pleiotropic effect of HDAC9 in cardiovascular diseases.

4.6 Clinical Implications of HDAC9 Inhibition

Accumulating evidence consistently consolidates the expanding clinical role of each proinflammatory molecule studied in this thesis in atherosclerosis. A prime example is how analysis of human serum demonstrated IL-8 to independently predict cardiovascular events[40]. Furthermore, a recent patient study revealed a genetic predisposition for elevated circulating levels of CCL2/MCP-1 to be associated with higher risk for large vessel and cardioembolic stroke[43]. Concurrently, our findings reveal how HDAC9 deficiency reduces CCL2/MCP-1 and IL-8 production in resident vascular cell. (Figure 8) Moreover, we carried out Hdac9 depletion in an animal atherosclerosis model and showed significantly lower levels of CCL2/MCP-1 compared to control just after 8 weeks being fed a lipid-rich diet. (Figure 9) Therefore, aligning our results to existing data shows that decreasing circulating levels of these two molecules could potentially delay atherosclerotic plaque development and subsequent onset of stroke[43,45]. This evidence points to the critical role of HDAC9 in the initiation and early-stage development of vascular inflammation. More importantly, data shown here strongly supports the implementation of targeted HDAC9 inhibition as primary prophylaxis for stroke risk reduction. Current secondary prevention of recurrent ischemic events in stroke patients involves the use of simvastatin, which aside from reducing serum lipid-levels also decreases IL-8 production[45]. Hence, suppressing HDAC9 could similarly benefit patients and prevent them from having a repeated cerebrovascular event.

Upon reviewing existing clinical approaches, we encountered broad spectrum HDAC inhibitors in cancer and anti-seizure therapy[86,87]. However, currently available HDACis like TSA are unspecific and demonstrate contradictory results in ECs[80,81]. Interestingly, a recent study from our group revealed a specific Class IIa HDACi, TMP195, to attenuate p65 phosphorylation and inhibit pro-inflammatory responses *in vivo*[89]. These novel findings suggest that elucidating the role of HDAC9 and other individual HDACs could be beneficial in developing specific high-prospect therapy approaches for treating vascular inflammation in patients.

Finally, it is important to note that the cell-type specific role of HDACis is also poorly understood. For example, broad spectrum HDAC inhibitor TSA even exacerbated atherosclerotic lesion size, despite its atheroprotective effects in macrophages[81,85]. In contrast, we managed to demonstrate coherent anti-inflammatory effects in vascular resident cells and macrophages with reduced HDAC9 levels. Due to these synergistic effects across all three main cell-types involved in atherosclerosis, it is possible to conclude that blocking HDAC9 production could significantly delay atherosclerotic plaque formation in humans.

5 Conclusion

Previous studies already suggested HDAC9 as a potential drug target for atherosclerosis and stroke prevention[21]. The results of this thesis identified ECs and VSMCs to be responsible for the atheroprotective effect of HDAC9 deficiency. A combined effect of these cell types caused reduced expression of proatherogenic molecules in vitro and in $Hdac9^{-/-}Apoe^{-/-}$ mice. (Figure 8, 9)

Moreover, we were able to identify NF-κB as the underlying pathway by which HDAC9 induces atherogenic processes. Although we demonstrated HDAC9 to directly interact with IKKβ and affect its catalytic activity in a recent publication, it is highly probably that due to the complexity of the NF-κB pathway other non-histone proteins may be similarly affected by HDAC9 interaction[53,89]. In fact just as existing evidence demonstrated with other HDACs, it is also possible for atherosclerosis phenotype induced by HDAC9 to be caused by altered efficacy of NF-κB to DNA binding, changed recruitment of co-activators and other HDACs or increased inhibition of co-repressors.

While discoveries in this thesis further expand our understanding of HDAC9 role in atherosclerosis, multiple studies showed effects of reduced HDAC9 expression to be contradictory across different tissue types[85]. Contrary to our findings, Hdac9-deficiency was even shown to worsen ischemic stroke outcome and neuronal survival in mice[82]. Hence, further research is required to elucidate HDAC9-mediated mechanisms in NF-κB signaling. Understanding these intricate molecular interactions is a fundamental step for developing a pharmacological compound with high tissue-specificity suitable for successful clinical use[88].

References

1. Donkor ES. Stroke in the 21st Century: A Snapshot of the Burden, Epidemiology, and Quality of Life. Stroke Res Treat. 2018 Nov 27:2018:3238165

2. Murray CJ, Vos T, Lozano R, Naghavi M, Flaxman AD, Michaud C, Ezzati M, Shibuya K, Salomon JA, Abdalla S, Aboyans V, Abraham J, Ackerman I, Aggarwal R, Ahn SY, et al. (2012). Disability-adjusted life years (DALYs) for 291 diseases and injuries in 21 regions, 1990-2010: a systematic analysis for the Global Burden of Disease Study 2010. Lancet. 380(9859):2197-2223

3. Lozano R, Naghavi M, Foreman K, Lim S, Shibuya K, Aboyans V, Abraham J, Adair T, Aggarwal R, Ahn SY, Alvarado M, Anderson HR, Anderson LM, Andrews KG, Atkinson C, et al. (2012). Global and regional mortality from 235 causes of death for 20 age groups in 1990 and 2010: a systematic analysis for the Global Burden of Disease Study 2010. Lancet. 380(9859):2095-2128

4. Kissela BM, Khoury JC, Alwell K, Moomaw CJ, Woo D, Adeoye O, Flaherty ML, Khatri P, Ferioli S, De Los Rios La Rosa F, Broderick JP, Kleindorfer DO. Age at stroke: temporal trends in stroke incidence in a large, biracial population. Neurology. 2012 Oct 23;79(17):1781-7

5. Feigin VL, Forouzanfar MH, Krishnamurthi R, Mensah GA, Connor M, Bennett DA, Moran AE, Sacco RL, Anderson L, Truelsen T, O'Donnell M, Venketasubramanian N, Barker-Collo S, Lawes CM, Wang W, et al. (2014). Global and regional burden of stroke during 1990-2010: findings from the Global Burden of Disease Study 2010. Lancet. 383(9913):245-254

6. Luengo-Fernandez R, Violato M, Candio P, Leal J. Economic burden of stroke across Europe: A population-based cost analysis. Eur Stroke J. 2020 Mar;5(1):17-25

7. Olesen J, Gustavsson A, Svensson M, Wittchen HU, Jonsson B (2012). The economic cost of brain disorders in Europe. Eur J Neurol. 19(1):155-162

8. O'Donnell MJ, Chin SL, Rangarajan S, Xavier D, Liu L, Zhang H, Rao-Melacini P, Zhang X, Pais P, Agapay S, Lopez-Jaramillo P, Damasceno A, Langhorne P, McQueen MJ, Rosengren A, Dehghan M, Hankey GJ, Dans AL, Elsayed A, Avezum A, Mondo C, Diener HC, Ryglewicz D, Czlonkowska A, Pogosova N, Weimar C, Iqbal R, Diaz R, Yusoff K, Yusufali A, Oguz A, Wang X, Penaherrera E, Lanas F, Ogah OS, Ogunniyi A, Iversen HK, Malaga G, Rumboldt Z, Oveisgharan S, Al Hussain F, Magazi D, Nilanont Y, Ferguson J, Pare G, Yusuf S; INTERSTROKE investigators. Global and regional effects of potentially modifiable risk factors associated with acute stroke in 32 countries (INTERSTROKE): a case-control study. Lancet. 2016 Aug 20;388(10046):761-75

9. Kolominsky-Rabas PL, Weber M, Gefeller O, Neundoerfer B, Heuschmann PU. Epidemiology of ischemic stroke subtypes according to TOAST criteria: incidence, recurrence, and long-term survival in ischemic stroke subtypes: a population-based study. Stroke.2001 Dec 1;32(12):2735-40

10. Adams HP, Jr., Bendixen BH, Kappelle LJ, Biller J, Love BB, Gordon DL, Marsh EE, 3rd (1993). Classification of subtype of acute ischemic stroke. Definitions for use in a multicenter clinical trial. TOAST. Trial of Org 10172 in Acute Stroke Treatment. Stroke. 24(1):35-41

11. Bevan S, Traylor M, Adib-Samii P, Malik R, Paul NL, Jackson C, Farrall M, Rothwell PM, Sudlow C, Dichgans M, Markus HS (2012). Genetic heritability of ischemic stroke and the contribution of previously reported candidate gene and genome-wide associations. Stroke. 43(12):3161-3167

12. Traylor M, Farrall M, Holliday EG, Sudlow C, Hopewell JC, Cheng YC, Fornage M, Ikram MA, Malik R, Bevan S, Thorsteinsdottir U, Nalls MA, Longstreth W, Wiggins KL, Yadav S, et al. (2012). Genetic risk factors for ischemic stroke and its subtypes (the METASTROKE collaboration): a meta-analysis of genome-wide association studies. Lancet Neurol. 11(11):951-962

13. Dichgans M, Pulit SL, Rosand J. Stroke genetics: discovery, biology, and clinical applications. Lancet Neurol. 2019 Jun;18(6):587-599

14. Hirschhorn JN, Lohmueller K, Byrne E, Hirschhorn K (2002). A comprehensive review of genetic association studies. Genet Med. 4(2):45-61

15. Deloukas P, Kanoni S, Willenborg C, Farrall M, Assimes TL, Thompson JR, Ingelsson E, Saleheen D, Erdmann J, Goldstein BA, Stirrups K, Konig IR, Cazier JB, Johansson A, Hall AS, et al. (2013). Large-scale association analysis identifies new risk loci for coronary artery disease. Nat Genet. 45(1):25-33

16. Dichgans M, Malik R, Konig IR, Rosand J, Clarke R, Gretarsdottir S, Thorleifsson G, Mitchell BD, Assimes TL, Levi C, O'Donnell CJ, Fornage M, Thorsteinsdottir U, Psaty BM, Hengstenberg C, et al. (2014). Shared genetic susceptibility to ischemic stroke and coronary artery disease: a genome- wide analysis of common variants. Stroke. 45(1):24-36

17. Bellenguez C, Bevan S, Gschwendtner A, Spencer CC, Burgess AI, Pirinen M, Jackson CA, Traylor M, Strange A, Su Z, Band G, Syme PD, Malik R, Pera J, Norrving B, et al. (2012). Genome-wide association study identifies a variant in HDAC9 associated with large vessel ischemic stroke. Nat Genet. 44(3):328-333

18. International Stroke Genetics C, Welcome Trust Case Control C, Bellenguez C, et al. Genome-wide association study identifies a variant in hdac9 associated with large vessel ischemic stroke. Nature genetics.2012;44:328-333

19. Malik R, Chauhan G, Traylor M, Sargurupremraj M, Okada Y, Mishra A, Rutten-Jacobs L, Giese AK, van der Laan SW, …., Markus HS, Howson JMM, Kamatani Y, Debette S, Dichgans M. Multiancestry genome-wide association study of 520,000 subjects identifies 32 loci associated with stroke and stroke subtypes. Nat Genet. 2018 Apr;50(4):524-537

20. Markus HS, Makela KM, Bevan S, Raitoharju E, Oksala N, Bis JC, O'Donnell C, Hainsworth A, Lehtimaki T. Evidence hdac9 genetic variant associated with ischemic stroke increases risk via promoting carotid atherosclerosis. Stroke. 2013: 44:1220- 1225

21. Azghandi S, Prell C, van der Laan SW, Schneider M, Malik R, Berer K, Gerdes N, Pasterkamp G, Weber C, Haffner C, Dichgans M. Deficiency of the stroke relevant hdac9

gene attenuates atherosclerosis in accord with allele-specific effects at 7p21.1. Stroke. 2015;46:197-202

22. Lusis AJ (2000). Atherosclerosis. Nature. 407(6801):233-241

23. Hansson GK (2005). Inflammation, atherosclerosis, and coronary artery disease. N Engl J Med. 352(16):1685-1695

24. Wick G, Knoflach M, Xu Q. Autoimmune and inflammatory mechanisms in atherosclerosis. Annu Rev Immunol 2004;22:361–403

25. Ross R. Atherosclerosis—an inflammatory disease. N Engl J Med 1999;340:115–126

26. Ross R, Harker L (1976). Hyperlipidemia and atherosclerosis. Science. 193(4258):1094-1100

27. Lee DY, Chiu JJ. Atherosclerosis and flow: roles of epigenetic modulation in vascular endothelium. J Biomed Sci. 2019 Aug 7;26(1):56

28. Skalen K, Gustafsson M, Rydberg EK, Hulten LM, Wiklund O, Innerarity TL, Boren J (2002). Subendothelial retention of atherogenic lipoproteins in early atherosclerosis. Nature. 417(6890):750-754

29. Garcia-Ramallo E, Marques T, Prats N, Beleta J, Kunkel SL, Godessart N. Resident cell chemokine expression serves as the major mechanism for leukocyte recruitment during local inflammation. Journal of immunology. 2002;169:6467-6473

30. Jonasson L, Holm J, Skalli O, Bondjers G, Hansson GK (1986). Regional accumulations of T cells, macrophages, and smooth muscle cells in the human atherosclerotic plaque. Arteriosclerosis. 6(2):131-138

31. Weber C, Noels H. Atherosclerosis: Current pathogenesis and therapeutic options. Nature medicine. 2011;17:1410-1422

32. Weber, C., Zernecke, A. & Libby, P. The multifaceted contributions of leukocyte subsets to atherosclerosis: lessons from mouse models. *Nat Rev Immunol* 8. 2008:802–815

33. Finn AV, Nakano M, Narula J, Kolodgie FD, Virmani R (2010). Concept of vulnerable/unstable plaque. Arterioscler Thromb Vasc Biol. 30(7):1282-1292

34. Bennett MR, Sinha S, Owens GK. Vascular Smooth Muscle Cells in Atherosclerosis. *Circ Res*. 2016;118(4):692-702

35. Maskrey BH, Megson IL, Whitfield PD, Rossi AG. Mechanisms of resolution of inflammation: A focus on cardiovascular disease. Arterioscler Thromb Vasc Biol. 2011;31:1001-1006

36. de Winther MP, Kanters E, Kraal G, Hofker MH. Nuclear factor kappa b signaling in atherogenesis. Arteriosclerosis, thrombosis, and vascular biology. 2005;25:904-914

37. Garcia-Ramallo E, Marques T, Prats N, Beleta J, Kunkel SL, Godessart N. Resident cell chemokine expression serves as the major mechanism for leukocyte recruitment during local inflammation. Journal of immunology. 2002;169:6467-6473

38. Cybulsky MI, Iiyama K, Li H, Zhu S, Chen M, Iiyama M, Davis V, Gutierrez-Ramos JC, Connelly PW, Milstone DS (2001). A major role for VCAM-1, but not ICAM-1, in early atherosclerosis. J Clin Invest. 107(10):1255-1262

39. Kitagawa K, Matsumoto M, Sasaki T, Hashimoto H, Kuwabara K, Ohtsuki T, Hori M. Involvement of ICAM-1 in the progression of atherosclerosis in ApoE-knockout mice. Atherosclerosis. 2002 Feb;160(2):305-10

40. Apostolakis S, Vogiatzi K, Amanatidou V, Spandidos DA. Interleukin 8 and cardiovascular disease. Cardiovasc Res. 2009 Dec 1;84(3):353-60

41. Gu L, Okada Y, Clinton SK, Gerard C, Sukhova GK, Libby P, Rollins BJ (1998). Absence of monocyte chemoattractant protein-1 reduces atherosclerosis in low density lipoprotein receptor-deficient mice. Mol Cell. 2(2): 275-281

42. Lin J, Kakkar V, Lu X. Impact of MCP-1 in atherosclerosis. Curr Pharm Des. 2014;20(28):4580-8

43. Georgakis MK, Malik R, Björkbacka H, Pana TA, Demissie S, Ayers C, Elhadad MA, Fornage M, Beiser AS, Benjamin EJ, Boekholdt SM, Engström G, Herder C, Hoogeveen RC, Koenig W, Melander O, Orho-Melander M, Schiopu A, Söderholm M, Wareham N, Ballantyne CM, Peters A, Seshadri S, Myint PK, Nilsson J, de Lemos JA, Dichgans M. Circulating Monocyte Chemoattractant Protein-1 and Risk of Stroke: Meta-Analysis of Population-Based Studies Involving 17 180 Individuals. Circ Res. 2019 Sep 27;125(8):773-782

44. Yue TL, Wang X, Sung CP, Olson B, McKenna PJ, Gu JL, Feuerstein GZ. Interleukin-8. A mitogen and chemoattractant for vascular smooth muscle cells. Circ Res. 1994 Jul;75(1):1-7

45. Ito T, Ikeda U, Yamamoto K, Shimada K. Regulation of interleukin-8 expression by HMG-CoA reductase inhibitors in human vascular smooth muscle cells. Atherosclerosis. 2002 Nov;165(1):51-5

46. Newby AC, Zaltsman AB. Fibrous cap formation or destruction--the critical importance of vascular smooth muscle cell proliferation, migration and matrix formation. Cardiovasc Res. 1999;41:345–360

47. Heldin CH, Westermark B, Wasteson A. Platelet-derived growth factor. Isolation by a large-scale procedure and analysis of subunit composition. Biochem J. 1981;193:907–913

48. Sano H, et al. Functional blockade of platelet-derived growth factor receptor-beta but not of receptor-alpha prevents vascular smooth muscle cell accumulation in fibrous cap lesions in apolipoprotein E-deficient mice. Circulation. 2001;103:2955–2960

49. He C, Medley SC, Hu T, Hinsdale ME, Lupu F, Virmani R, Olson LE. PDGFRβ signaling regulates local inflammation and synergizes with hypercholesterolemia to promote atherosclerosis. Nat Commun. 2015 Jul 17;6:7770

50. Hariri RJ, Hajjar DP, Coletti D, Alonso DR, Weksler ME, Rabellino E. Aging and arteriosclerosis. Cell cycle kinetics of young and old arterial smooth muscle cells. Am J Pathol. 1988;131:132–136

51. Gomez D, Owens GK. Smooth muscle cell phenotypic switching in atherosclerosis. Cardiovasc Res. 2012;95:156–164

52. Tanya D Izzard, Christine Taylor, Sonia D Birkett, Christopher L Jackson, Andrew C Newby, Mechanisms underlying maintenance of smooth muscle cell quiescence in rat aorta: role of the cyclin dependent kinases and their inhibitors, *Cardiovascular Research*, Volume 53, Issue 1, January 2002, Pages 242–252

53. Hayden MS, Ghosh S. Regulation of NF-κB by TNF family cytokines. Semin Immunol. 2014 Jun;26(3):253-66

54. Barnes PJ, Karin M. Nuclear factor-kappaB: a pivotal transcription factor in chronic inflammatory diseases. N Engl J Med. 1997 Apr 10;336(15):1066-71

55. Richmond A. Nf-kappa b, chemokine gene transcription and tumour growth. Nature reviews. Immunology. 2002;2:664-674

56. Chen L, Fischle W, Verdin E, Greene WC. Duration of nuclear nf-kappab action regulated by reversible acetylation. Science. 2001;293:1653-1657

57. Yang S, Xie C, Chen Y, Wang J, Chen X, Lu Z, June RR, Zheng SG. Differential roles of TNFα-TNFR1 and TNFα-TNFR2 in the differentiation and function of $CD4^{+}Foxp3^{+}$ induced Treg cells in vitro and in vivo periphery in autoimmune diseases. Cell Death Dis. 2019 Jan 10;10(1):27

58. Sun SC, Ganchi PA, Ballard DW, Greene WC. Nf-kappa b controls expression of inhibitor i kappa b alpha: Evidence for an inducible autoregulatory pathway. Science. 1993;259:1912-1915

59. Christian F, Smith EL, Carmody RJ. The regulation of nf-kappab subunits by phosphorylation. Cells. 2016;5

60. Ashburner BP, Westerheide SD, Baldwin AS, Jr. The p65 (rela) subunit of nf-kappab interacts with the histone deacetylase (hdac) corepressors hdac1 and hdac2 to negatively regulate gene expression. Molecular and cellular biology. 2001;21:7065-7077

61. Chaturvedi MM, Sung B, Yadav VR, Kannappan R, Aggarwal BB. NF-κB addiction and its role in cancer: 'one size does not fit all'. Oncogene. 2011 Apr 7;30(14):1615-30

62. Moreno R, Sobotzik JM, Schultz C, Schmitz ML. Specification of the nf-kappab transcriptional response by p65 phosphorylation and tnf-induced nuclear translocation of ikk epsilon. Nucleic acids research. 2010;38:6029-6044

63. Zhong H, May MJ, Jimi E, Ghosh S. The phosphorylation status of nuclear nf-kappa b determines its association with cbp/p300 or hdac-1. Molecular cell. 2002;9:625-636

64. Kyriakis JM, Avruch J. Mammalian MAPK signal transduction pathways activated by stress and inflammation: a 10-year update. Physiol Rev. 2012;92:689–737

65. Enslen H, Davis RJ. Regulation of MAP kinases by docking domains. Biol Cell. 2001;93:5–14

66. Sabio G, Davis RJ. TNF and MAP kinase signaling pathways. *Semin Immunol*. 2014;26(3):237-245

67. Das S, Cho J, Lambertz I, Kelliher MA, Eliopoulos AG, Du K, Tsichlis PN. Tpl2/cot signals activate ERK, JNK, and NF-kappaB in a cell-type and stimulus-specific manner. J Biol Chem. 2005;280:23748–57

68. Gantke T, Sriskantharajah S, Sadowski M, Ley SC. IkappaB kinase regulation of the TPL-2/ERK MAPK pathway. Immunol Rev. 2012;246:168–82

69. Yang HT, Papoutsopoulou S, Belich M, Brender C, Janzen J, Gantke T, Handley M, Ley SC. Coordinate regulation of TPL-2 and NF-kappaB signaling in macrophages by NF-kappaB1 p105. Mol Cell Biol. 2012;32:3438–51

70. Davis RJ. Signal transduction by the JNK group of MAP kinases. Cell. 2000;103:239–52

71. Cuadrado A, Nebreda AR. Mechanisms and functions of p38 MAPK signalling. Biochem J. 2010;429:403–17

72. Sakurai H. Targeting of TAK1 in inflammatory disorders and cancer. Trends Pharmacol Sci. 2012;33:522–30

73. Gallo KA, Johnson GL. Mixed-lineage kinase control of JNK and p38 MAPK pathways. Nat Rev Mol Cell Biol. 2002;3:663–72

74. Allfrey VG, Faulkner R, Mirsky AE (1964). Acetylation and Methylation of Histones and Their Possible Role in the Regulation of Rna Synthesis. Proc Natl Acad Sci U S A. 51:786-794

75. Haberland M, Montgomery RL, Olson EN (2009). The many roles of histone deacetylases in development and physiology: implications for disease and therapy. Nat Rev Genet. 10(1):32-42

76. Shahbazian MD, Grunstein M (2007). Functions of site-specific histone acetylation and deacetylation. Annu Rev Biochem. 76:75-100

77. Falkenberg KJ, Johnstone RW (2014). Histone deacetylases and their inhibitors in cancer, neurological diseases and immune disorders. Nat Rev Drug Discov. 13(9):673-691

78. Zheng XX, Zhou T, Wang XA, Tong XH, Ding JW. Histone deacetylases and atherosclerosis. Atherosclerosis. 2015;240:355-366 Zhou B, Margariti A, Zeng L, Xu Q. Role of histone deacetylases in vascular cell homeostasis and arteriosclerosis. Cardiovasc Res. 2011 Jun 1;90(3):413-20

79. McKinsey TA, Zhang CL, Lu J, Olson EN (2000). Signal-dependent nuclear export of a histone deacetylase regulates muscle differentiation. Nature. 408(6808): 106-111

80. Zampetaki A, Zeng L, Margariti A, Xiao Q, Li H, Zhang Z, Pepe AE, Wang G, Habi O, deFalco E, Cockerill G, Mason JC, Hu Y, Xu Q. Histone deacetylase 3 is critical in endothelial survival and atherosclerosis development in response to disturbed flow. Circulation.2010;121:132-142

81. Hoeksema MA, Gijbels MJ, Van den Bossche J, van der Velden S, Sijm A, Neele AE, Seijkens T, Stoger JL, Meiler S, Boshuizen MC, Dallinga-Thie GM, Levels JH, Boon L, Mullican SE, Spann NJ, Cleutjens JP, Glass CK, Lazar MA, de Vries CJ, Biessen EA, Daemen MJ, Lutgens E, de Winther MP. Targeting macrophage histone deacetylase 3 stabilizes atherosclerotic lesions. EMBO molecular medicine.2014;6:1124-1132

82. Kim HJ, Rowe M, Ren M, Hong JS, Chen PS, Chuang DM (2007). Histone deacetylase inhibitors exhibit anti-inflammatory and neuroprotective effects in a rat permanent ischemic model of stroke: multiple mechanisms of action. J Pharmacol Exp Ther. 321(3):892-901

83. Morrison BE, Majdzadeh N, Zhang X, Lyles A, Bassel-Duby R, Olson EN, D'Mello SR (2006). Neuroprotection by histone deacetylase-related protein. Mol Cell Biol. 26(9): 3550-3564

84. Shein NA, Shohami E (2011). Histone deacetylase inhibitors as therapeutic agents for acute central nervous system injuries. Mol Med. 17(5-6):448-456

85. Shakespear MR, Halili MA, Irvine KM, Fairlie DP, Sweet MJ. Histone deacetylases as regulators of inflammation and immunity. Trends in immunology. 2011;32:335-343

86. Marks PA, Breslow R (2007). Dimethyl sulfoxide to vorinostat: development of this histone deacetylase inhibitor as an anticancer drug. Nat Biotechnol. 25(1):84-90

87. Marson AG, Al- Kharusi AM, Alwaidh M, Appleton R, Baker GA, Chadwick DW, Cramp C, Cockerell OC, Cooper PN, Doughty J, Eaton B, Gamble C, Goulding PJ, Howell SJ, Hughes A, et al. (2007). The SANAD study of effectiveness of valproate, lamotrigine, or topiramate for generalised and unclassifiable epilepsy: an unblinded randomised controlled trial. Lancet. 369(9566):1016-1026

88. Di Giorgio E, Gagliostro E, Brancolini C. Selective class iia hdac inhibitors: Myth or reality. Cellular and molecular life sciences : CMLS. 2015;72:73-86

89. Asare Y, Campbell-James TA, Bokov Y, Yu LL, Prestel M, El Bounkari O, Roth S, Megens RTA, Straub T, Thomas K, Yan G, Schneider M, Ziesch N, Tiedt S, Silvestre-Roig C, Braster Q, Huang Y, Schneider M, Malik R, Haffner C, Liesz A, Soehnlein O, Bernhagen J, Dichgans M. Histone Deacetylase 9 Activates IKK to Regulate Atherosclerotic Plaque Vulnerability. Circ Res. 2020 Aug 28;127(6):811-823

90. Gray SG, Ekstrom TJ. The human histone deacetylase family. Exp Cell Res 2001;262:75–83

91. Cao Q, Rong S, Repa JJ, Clair RS, Parks JS, Mishra N (2014). Histone deacetylase 9 represses cholesterol efflux and alternatively activated macrophages in atherosclerosis development. Arterioscler Thromb Vasc Biol. 34(9):1871-1879

92. Malhotra R, Mauer AC, Lino Cardenas CL, Guo X, Yao J, Zhang X, et. al. HDAC9 is implicated in atherosclerotic aortic calcification and affects vascular smooth muscle cell phenotype. Nat Genet. 2019 Nov;51(11):1580-1587

93. Han X, Han X, Wang Z, Shen J, Dong Q. HDAC9 regulates ox-LDL-induced endothelial cell apoptosis by participating in inflammatory reactions. Front Biosci (Landmark Ed). 2016 Jun 1;21:907-17

94. de Zoeten EF, Wang L, Sai H, Dillmann WH, Hancock WW. Inhibition of HDAC9 increases T regulatory cell function and prevents colitis in mice. Gastroenterology. 2010 Feb;138(2):583-94

95. Li X, Zhang Q, Ding Y, Liu Y, Zhao D, Zhao K, Shen Q, Liu X, Zhu X, Li N, ChengZ, Fan G, Wang Q, Cao X. Methyltransferase dnmt3a upregulates hdac9 to deacetylate the kinase tbk1 for activation of antiviral innate immunity. Nature immunology. 2016; 17:806-815

96. Getz GS, Reardon CA (2012). Animal models of atherosclerosis. Arterioscler Thromb Vasc Biol. 32(5):1104-1115

97. Plump AS, Smith JD, Hayek T, Aalto-Setala K, Walsh A, Verstuyft JG, Rubin EM, Breslow JL (1992). Severe hypercholesterolemia and atherosclerosis in apolipoprotein E-deficient mice created by homologous recombination in ES cells. Cell. 71(2):343-353

98. Getz GS, Reardon CA. Diet and murine atherosclerosis. Arterioscler Thromb Vasc Biol. 2006 Feb;26(2):242-9

Figure Legend

Acknowledgments

First and foremost, I would like to thank my supervisor Dr. Yaw Asare for his continued guidance, moral support, motivation and especially his patience during my time at ISD. I grew to value his continued interest in my academic progress long after completion of experimental work and thank him for our regular meetings that helped me stay up-to-date with the project.

I would also like to thank Prof. Dr. Martin Dichgans for the opportunity to work in his laboratory. I am very grateful for how open he was to any new ideas and how he was always excited to think out of the box. I appreciate the fruitful discussions and comments he provided on one-to-one basis and in our regular lab-meetings, which helped me tackle daily challenges in this project.

I am also grateful to the animal facility of the ISD for helping in management of *HDAC9* mouse lines. Special thanks to Melanie Schneider and Natalie Ziesch for all the technical support they gave me, but also for their very constructive comments and encouragement. Finally, I want to thank Farida for teaching me confocal microscopy and her readiness for any scientific discussions.

Thanks to my friends for supporting me and for always having time for me. I am enormously thankful to my parents and my siblings for their patience, motivation and love. Without them, this work would not have been possible. I cannot express enough the amount of gratefulness and love to my girlfriend Marie for her continued support and patience at all times.

Finally, I would like to thank all the proofreaders of this thesis.

LMU LUDWIG-MAXIMILIANS-UNIVERSITÄT MÜNCHEN

Promotionsbüro
Medizinische Fakultät

MMRS

Eidesstattliche Versicherung

Bokov, Yury

Name, Vorname

Ich erkläre hiermit an Eides statt,

dass ich die vorliegende Dissertation mit dem Titel

Role of the Large Vessel Stroke Relevant Gene HDAC9 in NF-kB Activation and Atherogenic Processes in Vascular Cells.

selbständig verfasst, mich außer der angegebenen keiner weiteren Hilfsmittel bedient und alle Erkenntnisse, die aus dem Schrifttum ganz oder annähernd übernommen sind, als solche kenntlich gemacht und nach ihrer Herkunft unter Bezeichnung der Fundstelle einzeln nachgewiesen habe.

Ich erkläre des Weiteren, dass die hier vorgelegte Dissertation nicht in gleicher oder in ähnlicher Form bei einer anderen Stelle zur Erlangung eines akademischen Grades eingereicht wurde.

München, 29.04.2022

Ort, Datum

Yury Bokov

Unterschrift Doktorandin bzw. Doktorand